# 藏南亚东地区早古生代花岗质片麻岩的成因与构造意义[*]

苟正彬[1,2]    张泽明[1**]    董昕[1]    丁慧霞[1]    向华[1]    雷恒聪[3]    李旺超[3]    唐磊[3]

GOU ZhengBin[1,2], ZHANG ZeMing[1**], DONG Xin[1], DING HuiXia[1], XIANG Hua[1], LEI HengCong[3], LI WangChao[3] and TANG Lei[3]

1. 中国地质科学院地质研究所,大陆构造与动力学国家重点实验室,北京    100037
2. 中国地质大学地球科学学院,武汉    430074
3. 中国地质大学地球科学与资源学院,北京    100083
1. *State Key Laboratory of Continental Tectonic and Dynamics, Institute of Geology, Chinese Academy of Geological Sciences, Beijing 100037, China*
2. *Faculty of Earth Sciences, China University of Geosciences, Wuhan 430074, China*
3. *School of Earth Science and Resources, China University of Geosciences, Beijing 100083, China*
2015-06-07 收稿, 2015-09-06 改回.

**Abstract**    Early Paleozoic granitic gneisses occur in the Higher Himalayan Crystallization Sequence of Yadong area, southern Tibet. Petrological study shows that the granitic gneisses are mainly composed of quartz, plagioclase, K-feldspar and biotite, and show distinct gneissic structure. They have variable $SiO_2$ contents ranging from 68.04% to 76.55%, and alumina saturation index (A/CNK) of 1.04 ~ 1.14, indicative of calcic to calc-alkaline and weakly peraluminous to peraluminous. They show distinct fractionated REE patterns with negative Eu anomalies, and are characterized by the enrichment of LILEs (such as Rb) and the depletion of HFSEs (such as Nb, Ta, P and Ti). LA-ICP-MS U-Pb dating of zircons from the three granitic gneisses indicates that their protoliths were formed at 491Ma, 501Ma and 512Ma, respectively. The zircon $\varepsilon_{Hf}(t)$ values range from −8.1 to +0.1, −5.9 to −2.1 and −4.8 to +6.7, with corresponding Hf two-stage model ages ranging from 1440Ma to 1959Ma, 1585Ma to 1826Ma and 1028Ma to 1762Ma, respectively. This study shows that the Early Paleozoic granites of Yadong area include I-type and S-type granitoids. The I-type granitoids are characterized by $K_2O/Na_2O$ (%) >1, weakly peraluminous, positive zircon $\varepsilon_{Hf}(t)$ values or negative but narrow $\varepsilon_{Hf}(t)$ values range, and show typical geochemical features of magmatic arcs. In contrast, minor S-type granites are characterized by $K_2O/Na_2O$ (%) <1, peraluminous, negative and variable zircon $\varepsilon_{Hf}(t)$ values. The coexistence of I-type and S-type granitoids in the Himalayas indicates that the northern margin of the Gondwana supercontinent experienced an Andean-type orogeny during the Early Paleozoic.

**Key words**    Granitic gneisses; Early Paleozoic; Himalaya; Andean-type orogeny; Gondwana

**摘    要**    早古生代的花岗质片麻岩产出在青藏高原南部亚东地区的高喜马拉雅结晶岩系中。岩石学研究表明,这些岩石主要由斜长石、钾长石、石英和黑云母组成,普遍发育片麻状构造。它们的 $SiO_2$ 含量为 68.04% ~ 76.55%,铝饱和指数(A/CNK)为 1.04 ~ 1.14,属钙性-钙碱性弱过铝-过铝质岩石。它们的稀土总量较高,轻稀土富集,Eu 负异常,富集大离子亲石元素 Rb,相对亏损 Nb、Ta、P 和 Ti 等高场强元素。三个样品获得的岩浆锆石 U-Pb 年龄分别为 491Ma、512Ma 和 501Ma,代表花岗质片麻岩的原岩年龄。它们的锆石 $\varepsilon_{Hf}(t)$ 值分别为 −8.1 ~ +0.1、−5.9 ~ −2.1 和 −4.8 ~ +6.7,对应的二阶段模式年龄分

别为 1440～1959Ma、1585～1826Ma 和 1028～1762Ma。本研究表明,亚东地区的早古生代花岗岩包括 I 型和 S 型花岗岩。I 型花岗岩以 $K_2O/Na_2O<1$、弱过铝质和刚玉标准矿物分子数 <1 为特征,具较高且正的锆石 $\varepsilon_{Hf}(t)$ 值,或相对集中的负的 $\varepsilon_{Hf}(t)$ 值。I 型花岗岩显示岩浆弧花岗岩的特征。S 型花岗岩以 $K_2O/Na_2O>1$、过铝质和刚玉标准矿物分子数 >1 为特征,锆石 $\varepsilon_{Hf}(t)$ 值均为低的负值,且变化范围较大。本文和现有的研究成果表明,I 型和 S 型花岗岩在喜马拉雅地体广泛存在,这为冈瓦纳超大陆北缘经历了早古生代的安第斯型造山作用提供了重要证据。

**关键词**　　　花岗质片麻岩;早古生代;喜马拉雅;安第斯型造山;冈瓦纳

**中图法分类号**　　　P588.345;P597.3

## 1　引言

　　位于喜马拉雅造山带核部的高级变质岩形成于印度与欧亚板块的碰撞过程中,是研究板块构造和大陆造山作用的理想对象,为大家所普遍关注(Rowley,1996;Yin and Harrison,2000;DeCelles et al.,2001;Ding et al.,2001;Mo et al.,2008;Hébert et al.,2012;Zhang et al.,2013,2014,2015)。最近的研究表明,造山带核部的高喜马拉雅结晶岩系经历了早古生代的构造热事件,普遍发育早古生代的花岗岩(Gehrels et al.,2003;Cawood and Buchan,2007;Cawood et al.,2007;董昕等,2009;时超等,2010;Wang et al.,2012a;Zhu et al.,2012;彭智敏等,2014;Ding et al.,2015)。尽管对这些发生在冈瓦纳大陆北缘的早古生代岩浆作用已经做了大量的研究,但对于它们的特征和成因还存在争议。此外,这些岩浆岩是形成在冈瓦纳大陆聚合引起的碰撞造山过程中(潘晓萍等,2012;Ding et al.,2015),还是与原特提斯洋向冈瓦纳大陆北缘俯冲导致的安第斯型造山有关也存在争议(Kusky et al.,2003;Cawood et al.,2007;董美玲等,2012;蔡志慧等,2013;Zhang et al.,2013)。以往的研究表明,花岗岩中锆石的 $\varepsilon_{Hf}(t)$ 值均为负值,由此获得古老的 Hf 二阶段模式年龄($t_{DM2}$)。因此,大家都认为它们是古老地壳物质部分熔融的产物(幸平阳等,2013;张士贞等,2014),目前还没有早古生代初生地壳部分熔融所形成花岗岩的报道。但是,Zhu et al.(2012)在拉萨地体中发现了490Ma 的基性岩,其锆石的 $\varepsilon_{Hf}(t)$ 值为高的正值,表明确实有早古生代的初生地壳物质。如果冈瓦纳大陆北缘经历了早古生代的安第斯型造山作用,就应该有由初生下地壳部分熔融形成的 I 型花岗岩形成。本文通过对藏南亚东地区高喜马拉雅结晶岩系中早古生代花岗质片麻岩的岩石学、锆石 U-Pb 年代学以及 Hf 同位素研究,揭示出这些岩石的地球化学特征,识别出了由古老地壳部分熔融形成的 S 型花岗岩和由初生下地壳部分熔融形成的 I 型花岗岩,为冈瓦纳大陆北缘的早古生代造山作用提供了新的信息。

## 2　区域地质背景和样品特征

　　青藏高原自北向南依次为松潘-甘孜杂地体、羌塘地体、拉萨地体和喜马拉雅地体(Yin and Harrison,2000),它们之间依次为金沙江、班公湖-怒江和雅鲁藏布江缝合带。喜马拉雅地体包含四个近平行的构造单元,从南到北依次为:次喜马拉雅单元、低喜马拉雅岩系、高喜马拉雅结晶岩系和特提斯喜马拉雅系列。它们之间分别以主边界逆冲断裂、主中央逆冲断裂和藏南拆离断裂为界(图1a)(Yin and Harrison,2000;许志琴等,2005)。次喜马拉雅单元由中新世到更新世的磨拉石组成。低喜马拉雅单元主要由一系列浅变质沉积岩组成,夹杂变质火山岩和眼球状片麻岩。高喜马拉雅结晶岩系是一个约30km 厚的中、高级变质岩系,主要由一套经历了角闪岩相-麻粒岩相变质的变质沉积岩和花岗质片麻岩组成,发育有少量的新生代花岗岩(Yin and Harrison,2000)。花岗质片麻岩的原岩年龄为早古生代(许志琴等,2005;张泽明等,2008,2013)。特提斯喜马拉雅带主要由低级变质的沉积岩组成,带内发育一系列的片麻岩穹窿和淡色花岗岩(Zeng et al.,2011;Hou et al.,2012)。

　　研究区位于藏南亚东县附近,构造上处于高喜马拉雅结晶岩系的上部构造层位(图1b)。该地区的高喜马拉雅结晶岩系主要由花岗质片麻岩(正片麻岩)、副片麻岩(变沉积岩)、泥质麻粒岩以及少量大理岩和钙硅酸岩组成。在印度与欧亚大陆的碰撞造山过程中,高喜马拉雅结晶岩系中的早古生代花岗岩与表壳岩一起遭受新生代的高级变质、部分熔融和强烈的变形改造。因此,由花岗岩转变而成的花岗质片麻岩发育片麻状构造和深熔脉体(图2a)。本文所研究的样品 20-1 采于中印边界(GPS 坐标为 27°25.9′N,88°53.7′E),样品 28-2 和 34-1 采自亚东县城西北方向约10km 的汤嘎西木(27°33.8′N,88°55.2′E 和 27°34.4′N,88°54.8′E;图1b)。混合岩化花岗质片麻岩由浅色的脉体和暗色的残留体组成,浅色体具鳞片粒状变晶结构,主要由石英(30%～35%)、斜长石(20%～25%)、钾长石(30%～35%)和少量黑云母(3%～5%)组成(图2b-d)。样品 20-1 和 34-1 中含有少量白云母(图2b,c),样品 28-2 中含少量角闪石(图2d)。定向分布的云母和角闪石,以及拉长的长石、石英或其集合体条带构成片麻理。

## 3　测试方法

　　全岩主量和微量元素化学成分分析在国家地质实验测试中心完成。主量元素分析采用 X-ray 荧光光谱法(XRF),仪器型号 Rigaku-3080,精度优于 0.5%,其中 FeO 采用容量
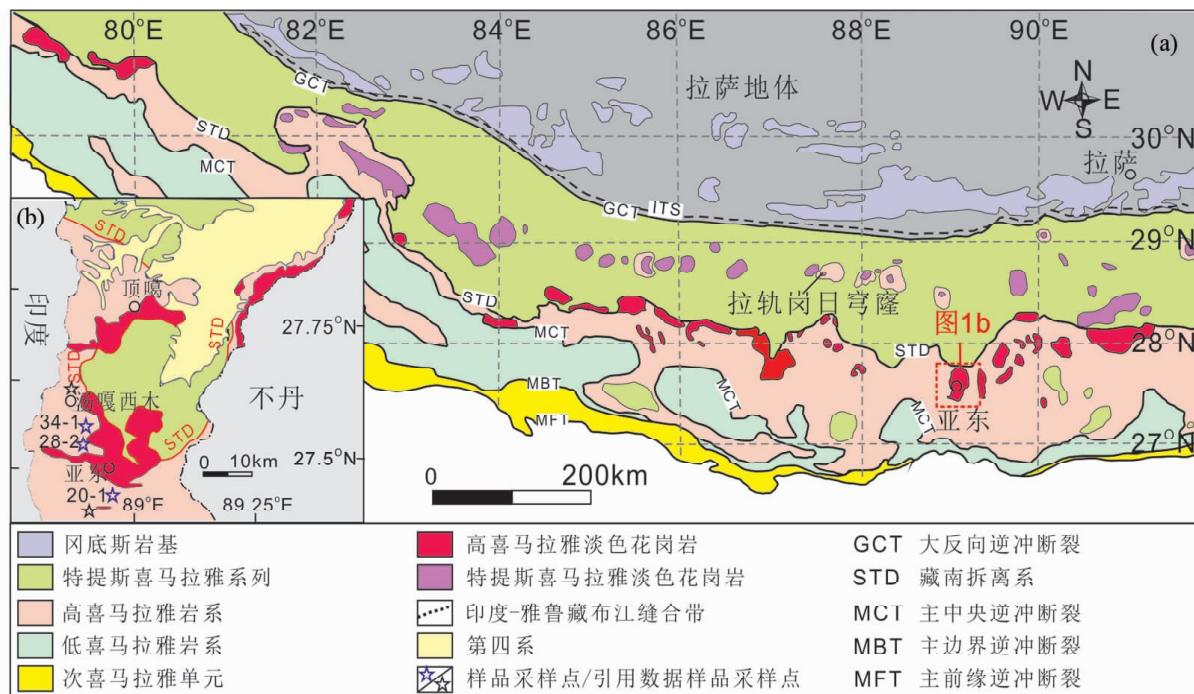
图 1    青藏高原南部地质简图(a,据 Guo and Wilson, 2012)和亚东地质简图(b)

Fig. 1    Simplified geological map of the southern Tibetan Plateau (a, after Guo and Wilson, 2012) and geological map of the Yadong area (b)
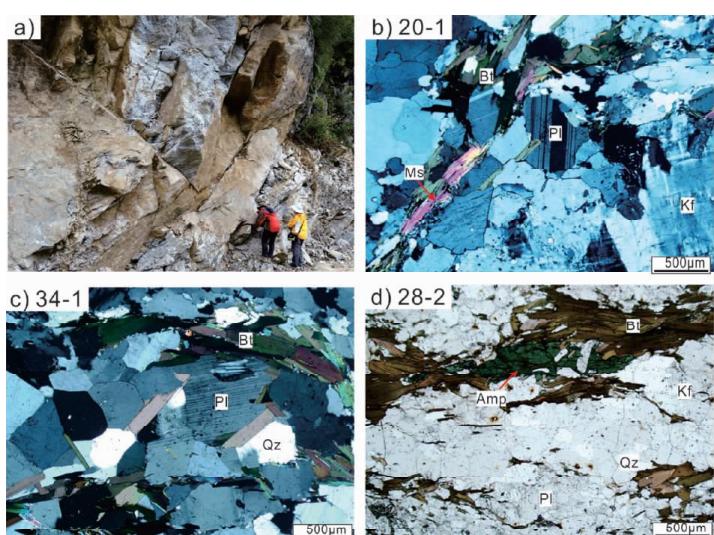


图 2    早古生代花岗质片麻岩野外照片及显微照片

Fig. 2    Photomicrographs of outcrops and photomicrographs of the Early Paleozoic granitic gneisses in Yadong area

滴定法。微量元素 Zr、Nb、V、Cr、Sr、Ba、Zn、Ni、Rb 和 Y 使用与测试主量元素不同的 XRF 设备(Rigaku-2100)进行分析,分析精度优于 3% ~ 5%。其他微量元素和稀土元素采用电感耦合等离子体质谱法(ICP-MS),当元素含量大于 $1 \times 10^{-6}$ 时,分析精度优于 1% ~ 5%,当元素含量小于 $1 \times 10^{-6}$ 时,分析精度优于 5% ~ 10%。

锆石 U-Pb 同位素定年在中国地质大学(武汉)地质过程与矿产资源国家重点实验室完成。测试仪器为 LA-ICP-MS,激光剥蚀系统为 GeoLas 2005,ICP-MS 为 Agilent 7500a。激光剥蚀斑束直径为 32μm,激光剥蚀深度为 20 ~ 40μm。对分

析数据的离线处理采用软件 ICPMSDataCal 完成。详细的仪器操作条件见 Liu et al. (2010),同位素数据结果处理使用 ISOPLOT 软件(Ludwig, 2003)完成。

锆石 Hf 同位素测试在中国地质科学院矿产资源研究所国土资源部成矿作用与资源评价重点实验室 Neptune 多接收等离子质谱和 Newwave UP213 紫外激光剥蚀系统 LA-MC-ICP-MS 上进行,分析采用的激光束斑直径为 55μm。实验过程中采用氦气作为剥蚀物质载气,锆石标准 GJ-1 作为参考,锆石 Lu-Hf 同位素测试点位于锆石 U-Pb 年龄测试点附近,采样方式为单点剥蚀。相关仪器运行条件及详细分析流程见侯可军等(2007)。分析过程中锆石标准 GJ-1 的 $^{176}Hf/^{177}Hf$ 测试加权平均值为 0.282008 ± 25,与 Elhlou et al. (2006)及侯可军等(2007)所报道的参考值在误差范围内一致。

# 4    岩石化学

本文所研究的 3 件花岗质片麻岩和已发表的亚东地区、邻近的拉轨岗日片麻岩穹窿中的早古生代花岗质片麻岩共 10 件样品一起讨论。它们的主量和微量元素成分分析结果已列于表 1。这些早古生代花岗质片麻岩的 $SiO_2$ 含量为 68.04% ~ 76.55%,$Al_2O_3$ 含量为 11.94% ~ 16.14%,全碱含量为 5.32% ~ 7.64%,但 FeO、MgO、MnO 和 $TiO_2$ 含量较低。岩石的里特曼指数($\sigma$)为 1.25 ~ 1.96,属钙性-钙碱性系列(图 3a)。这些花岗质片麻岩可分为两类:第一类包括本文样品 20-1 和拉轨岗日样品 L1 和 L2,它们的 $K_2O/Na_2O$ 为 1.27 ~ 2.02,铝饱和指数(A/CNK)为 1.14 ~ 1.19,CIPW 刚

表1 早古生代花岗质片麻岩的主量元素（wt%）和微量元素（×10⁻⁶）分析结果

Table 1 Major (wt%) and trace ($\times 10^{-6}$) element composition of the Early Paleozoic granitic gneisses

| 样品号 | 20-1 | L1 | L2 | 28-2 | 34-1 | Y1 | Y2 | Y3 | Y4 | Y5 |
|---|---|---|---|---|---|---|---|---|---|---|
| 岩石类型 | S 型 | | | I 型 | | | | | | |
| $SiO_2$ | 72.80 | 72.23 | 71.57 | 68.50 | 76.55 | 68.81 | 68.92 | 68.04 | 68.81 | 69.72 |
| $TiO_2$ | 0.42 | 0.64 | 1.07 | 0.44 | 0.12 | 0.48 | 0.49 | 0.50 | 0.37 | 0.41 |
| $Al_2O_3$ | 13.75 | 12.64 | 11.94 | 14.97 | 13.22 | 16.09 | 15.76 | 16.14 | 14.76 | 14.02 |
| $Fe_2O_3$ | 0.64 | 0.42 | 0.50 | 1.41 | 0.57 | 0.67 | 0.92 | 0.05 | 1.15 | 1.48 |
| FeO | 2.32 | 3.59 | 3.73 | 2.87 | 0.81 | 2.93 | 2.91 | 3.96 | 2.71 | 2.68 |
| MnO | 0.05 | 0.07 | 0.10 | 0.09 | 0.03 | 0.07 | 0.07 | 0.09 | 0.12 | 0.09 |
| MgO | 0.74 | 1.27 | 1.90 | 1.87 | 0.22 | 1.54 | 1.60 | 1.67 | 1.67 | 1.77 |
| CaO | 1.31 | 1.46 | 1.56 | 3.45 | 1.21 | 3.99 | 3.91 | 3.55 | 2.97 | 3.22 |
| $Na_2O$ | 2.53 | 2.33 | 2.38 | 3.05 | 4.05 | 3.42 | 3.22 | 3.64 | 3.46 | 2.92 |
| $K_2O$ | 5.11 | 3.79 | 3.02 | 2.59 | 3.29 | 1.92 | 2.10 | 2.27 | 2.83 | 2.53 |
| $P_2O_5$ | 0.08 | 0.14 | 0.13 | 0.09 | 0.03 | 0.09 | 0.09 | 0.09 | 0.09 | 0.10 |
| $CO_2$ | 0.26 | | | 0.17 | 0.17 | | | | 0.17 | 0.05 |
| $H_2O^+$ | 0.30 | | | 1.00 | 0.28 | | | | 0.72 | 0.78 |
| LOI | 0.23 | 1.48 | 1.66 | 0.63 | 0.27 | | | | 0.44 | 0.44 |
| Total | 99.75 | 100.06 | 99.55 | 99.33 | 100.10 | 100.01 | 99.99 | 100.00 | 98.94 | 98.94 |
| K/Na | 2.02 | 1.63 | 1.27 | 0.85 | 0.81 | 0.56 | 0.65 | 0.62 | 0.82 | 0.87 |
| A/CNK | 1.14 | 1.19 | 1.19 | 1.06 | 1.06 | 1.08 | 1.07 | 1.08 | 1.04 | 1.05 |
| A/NK | 1.42 | 1.59 | 1.66 | 1.91 | 1.29 | 2.09 | 2.08 | 1.91 | 1.69 | 1.86 |
| C | 1.87 | 1.26 | 1.20 | 0.88 | 0.80 | 0.94 | 0.93 | 0.96 | 0.73 | 0.77 |
| La | 27.3 | 48.3 | 98.4 | 29.2 | 29.3 | 47.9 | 31.7 | 52.8 | 42.8 | 21.1 |
| Ce | 58.7 | 89.2 | 183.9 | 58.1 | 58.6 | 80.8 | 55.2 | 90.0 | 77.4 | 39.9 |
| Pr | 6.8 | 10.7 | 21.2 | 6.4 | 6.3 | 9.1 | 6.4 | 10.0 | 7.9 | 4.5 |
| Nd | 25.0 | 40.4 | 79.3 | 23.6 | 21.9 | 31.7 | 23.4 | 34.5 | 30.9 | 19.3 |
| Sm | 5.9 | 9.4 | 16.0 | 4.6 | 4.5 | 5.9 | 4.9 | 6.0 | 5.5 | 4.4 |
| Eu | 0.8 | 1.2 | 1.5 | 1.1 | 0.7 | 1.3 | 1.2 | 1.2 | 1.2 | 1.0 |
| Gd | 6.0 | 8.9 | 13.0 | 4.7 | 4.9 | 4.6 | 4.0 | 4.5 | 4.9 | 4.6 |
| Tb | 1.1 | 1.4 | 1.8 | 0.8 | 0.9 | 0.7 | 0.6 | 0.6 | 0.8 | 0.8 |
| Dy | 6.2 | 9.3 | 9.4 | 4.1 | 5.4 | 3.8 | 3.6 | 3.1 | 4.2 | 4.1 |
| Ho | 1.2 | 1.9 | 1.7 | 0.8 | 1.1 | 0.7 | 0.7 | 0.6 | 0.8 | 0.8 |
| Er | 3.8 | 5.9 | 4.7 | 2.6 | 3.6 | 2.2 | 2.2 | 1.6 | 2.7 | 2.6 |
| Tm | 0.5 | 0.9 | 0.6 | 0.3 | 0.5 | 0.3 | 0.3 | 0.2 | 0.4 | 0.4 |
| Yb | 3.7 | 5.5 | 4.0 | 2.4 | 3.4 | 2.1 | 2.2 | 1.4 | 2.8 | 2.6 |
| Lu | 0.5 | 0.8 | 0.6 | 0.4 | 0.5 | 0.3 | 0.3 | 0.2 | 0.4 | 0.4 |
| $\Sigma REE$ | 147.5 | 288.8 | 481.3 | 139.0 | 141.5 | 191.4 | 136.7 | 206.7 | 182.6 | 106.2 |
| Eu/Eu* | 0.41 | 0.40 | 0.32 | 0.73 | 0.48 | 0.77 | 0.84 | 0.71 | 0.68 | 0.66 |
| $(La/Sm)_N$ | 2.81 | 3.25 | 3.86 | 3.92 | 4.00 | 4.95 | 3.95 | 5.37 | 4.71 | 2.96 |
| $(La/Yb)_N$ | 5.16 | 5.90 | 16.7 | 8.70 | 6.10 | 16.0 | 10.1 | 26.5 | 10.9 | 5.73 |
| $(La/Gd)_N$ | 3.86 | | | 5.21 | 5.09 | 8.78 | 6.68 | 9.89 | 7.35 | 3.88 |
| $(Gd/Yb)_N$ | 1.34 | 1.30 | 2.64 | 1.67 | 1.20 | 1.83 | 1.52 | 2.68 | 1.48 | 1.48 |
| Sc | 8.2 | 9.8 | 16.3 | 9.6 | 5.0 | 9.5 | 10.5 | 10.9 | 24.2 | 16.8 |
| V | 35.9 | | | 69.2 | 4.4 | 64.8 | 65.5 | 69.5 | 53.6 | 321.9 |
| Cr | 13.9 | 33.2 | 48.2 | 43.3 | 1.0 | 27.0 | 24.6 | 35.4 | 40.7 | 56.3 |
| Ni | 5.6 | 12.4 | 17.2 | 15.3 | <0.05 | 10.9 | 11.0 | 12.9 | <0.05 | <0.05 |
| Co | 5.6 | 153 | 176 | 11.1 | 1.3 | 149.6 | 186.0 | 137.9 | <0.05 | <0.05 |
| Rb | 295 | 256 | 218 | 119 | 148 | 120 | 125 | 152 | 233 | 129 |
| Sr | 65 | 63 | 69 | 215 | 76 | 270 | 262 | 241 | 61 | 201 |
| Y | 36.2 | 55.2 | 45.1 | 23.8 | 33.5 | 20.4 | 20.4 | 15.4 | 25.8 | 24.1 |
| Zr | 91 | 144 | 164 | 92 | 76 | 107 | 139 | 104 | 97 | 88 |
| Nb | 10.2 | 9.5 | 14.2 | 12.0 | 15.7 | 5.9 | 9.9 | 6.8 | 10.1 | 9.8 |
| Cs | 11.4 | | | 15.3 | 7.4 | 6.2 | 7.4 | 6.8 | 4.9 | 2.7 |
| Ba | 393 | 436 | 603 | 490 | 545 | 534 | 568 | 372 | 248 | 176 |
| Hf | 2.8 | 4.4 | 2.3 | 2.7 | 3.1 | 3.3 | 4.3 | 3.1 | 3.2 | 3.4 |
| Ta | 1.1 | 1.1 | 1.3 | 1.2 | 2.1 | 0.6 | 1.3 | 0.7 | 0.7 | 0.8 |
| Pb | 33.9 | | | 34.7 | 27.8 | 20.4 | 20.2 | 22.1 | 20.5 | 15.7 |
| Th | 21.4 | 29.8 | 55.6 | 15.3 | 18.3 | 15.8 | 14.9 | 26.2 | 16.0 | 17.8 |
| U | 5.0 | | | 2.2 | 3.7 | 1.5 | 1.7 | 4.6 | 1.4 | 3.2 |

注：L1 和 L2 据莘平阳等（2013）；Y1，Y2 和 Y3 据时超等（2010）；Y4 和 Y5 据中国地质大学（北京）地质调查研究院，2005[①]；其余为本文样品

① 中国地质大学（北京）地质调查研究院．2005. 1/25 万江孜县幅（H45C004004）、亚东县幅（G45C001004）（中国部分）区域地质调查报告
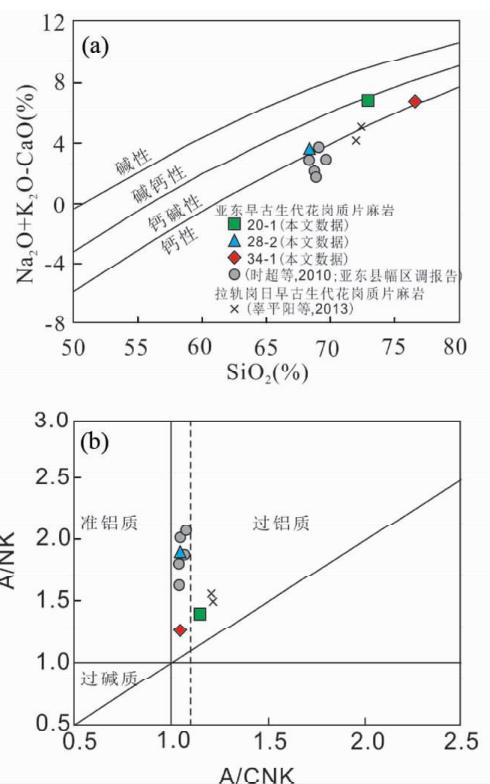
图3 花岗质片麻岩 $Na_2O + K_2O-CaO$ 与 $SiO_2$ 图解(a,据 Frost et al., 2001)和 A/NK-A/CNK 图解(b,据 Maniar and Piccoli, 1989)

Fig. 3 ($Na_2O + K_2O-CaO$) vs. $SiO_2$ plot (a, after Frost et al., 2001) and A/NK vs. A/CNK diagram (b, after Maniar and Piccoli, 1989) of the granitic gneisses

玉分子数大于1,属钾质过铝质岩石。第二类为本文的另2个样品和亚东地区已经发表的5个样品,它们的 $K_2O/Na_2O$ 为0.56~0.87,A/CNK 为1.04~1.08,CIPW 刚玉分子数小于1(表1),为钠质和弱过铝质岩石(图3b)。

所研究的早古生代花岗质片麻岩具有较高的稀土总量($106.2 \times 10^{-6} \sim 481.3 \times 10^{-6}$),在稀土元素球粒陨石标准化配分模式图中,轻重稀土元素分馏明显,轻稀土明显富集,$(La/Sm)_N$ 比值为2.81~5.37,$(La/Yb)_N$ 比值为5.16~26.5,$Eu/Eu^*$ 介于0.32~0.84之间,明显的负 Eu 异常(图4a)。在原始地幔标准化的微量元素蛛网图上,表现为富集大离子亲石元素 Rb,相对亏损 Nb、Ta、P 和 Ti 等高场强元素(图4b)。

# 5 锆石 U-Pb 定年和 Hf 同位素

## 5.1 锆石 U-Pb 年龄

3件花岗质片麻岩样品的锆石具有类似的特征,呈长柱状,长约100~300μm,长宽比为2~3。阴极发光图像显示这些锆石普遍具有核-边结构,即具有一个发育振荡环带的岩浆核和一个暗发光的5~10μm的增生边(图5)。样品20-1锆石岩浆核14个分析点给出的 $^{206}Pb/^{238}U$ 谐和年龄在464~491Ma之间(表2)。样品28-2锆石岩浆核13个分析点的 $^{206}Pb/^{238}U$ 年龄为470~512Ma之间;样品34-1锆石岩浆核13个分析点的 $^{206}Pb/^{238}U$ 年龄介于455~501Ma之间。这些分析点具有较高的 Th/U 比值(表2),稀土元素球粒陨石标准化配分曲线表现为明显的 HREE 富集,Ce 正异常,Eu 负异常的特点(图6和表3),为典型岩浆锆石的特征(Rubatto and Scambelluri, 2003);个别锆石显示了偏低的 Th/U 比值,可能与部分重结晶作用有关(Hoskin and Schaltegger, 2003; He et al., 2013)。由于这些花岗岩经历了新生代的高级变质作用,锆石的同位素体系很可能发生了部分重置,导致部分分
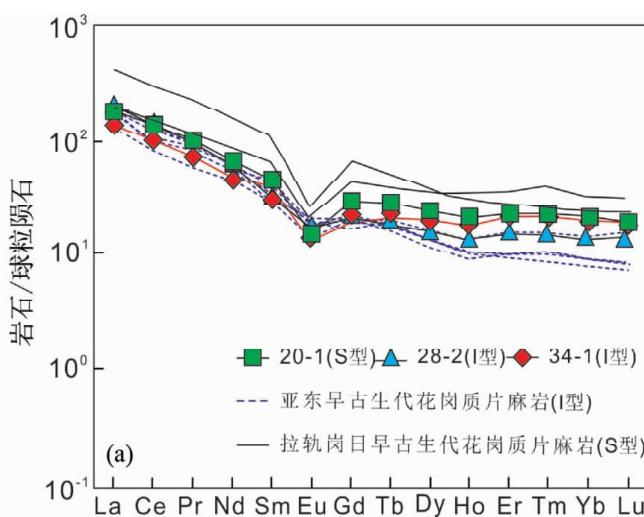


图4 稀土元素配分图(a,球粒陨石标准值据 Taylor and McLennan, 1985)和微量元素蛛网图(b,原始地幔标准值据 Sun and McDonough, 1989)

数据来源同图3

Fig. 4 Chondrite-normalized REE patterns (a, chondrite values after Taylor and McLennan, 1985) and primitive mantle-normalized trace element patterns (b, primitive mantle values after Sun and McDonough, 1989)

Data source are the same as in Fig. 3
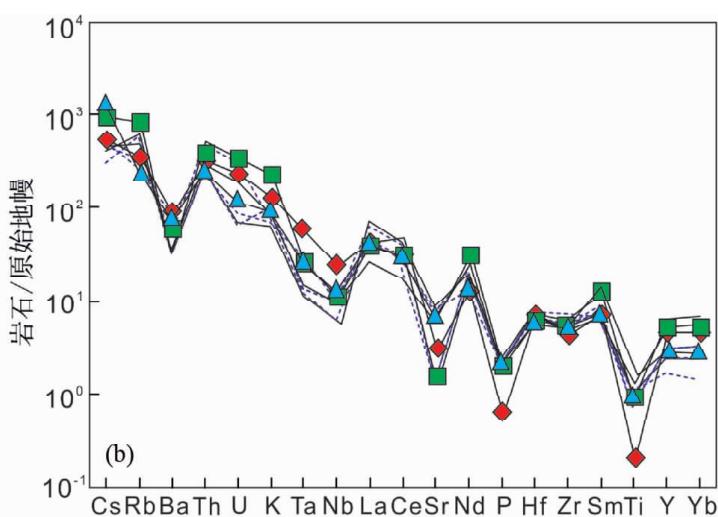
表2　研究区花岗质片麻岩 LA-ICPMS 锆石 U-Pb 定年结果

Table 2　LA-ICPMS zircon U-Pb data of the Early Paleozoic granitic gneisses

| Spot No. | Trace element ($\times 10^{-6}$) | | | Th/U | Isotopic ratio | | | | | | Age (Ma) | | | | | |
|---|---|---|---|---|---|---|---|---|---|---|---|---|---|---|---|---|
| | Pb | Th | U | | $\frac{^{207}Pb}{^{206}Pb}$ | ($\pm1\sigma$) | $\frac{^{207}Pb}{^{235}U}$ | ($\pm1\sigma$) | $\frac{^{206}Pb}{^{238}U}$ | ($\pm1\sigma$) | $\frac{^{207}Pb}{^{206}Pb}$ | ($\pm1\sigma$) | $\frac{^{207}Pb}{^{235}U}$ | ($\pm1\sigma$) | $\frac{^{206}Pb}{^{238}U}$ | ($\pm1\sigma$) |
| 20-1 花岗质片麻岩 | | | | | | | | | | | | | | | | |
| 20-1-02 | 68 | 68 | 779 | 0.09 | 0.0557 | 0.0011 | 0.5822 | 0.0112 | 0.0757 | 0.0007 | 439 | 42.6 | 466 | 7.2 | 470 | 4.4 |
| 20-1-04 | 75 | 88 | 763 | 0.12 | 0.0582 | 0.0012 | 0.6020 | 0.0153 | 0.0748 | 0.0012 | 600 | 48.1 | 479 | 9.7 | 465 | 7.2 |
| 20-1-06 | 136 | 110 | 1704 | 0.06 | 0.0571 | 0.0010 | 0.6045 | 0.0121 | 0.0764 | 0.0010 | 498 | 37.0 | 480 | 7.7 | 475 | 6.1 |
| 20-1-09 | 50 | 44 | 576 | 0.08 | 0.0578 | 0.0011 | 0.6199 | 0.0123 | 0.0779 | 0.0009 | 520 | 40.7 | 490 | 7.7 | 484 | 5.7 |
| 20-1-12 | 67 | 78 | 661 | 0.12 | 0.0583 | 0.0013 | 0.6162 | 0.0151 | 0.0764 | 0.0011 | 543 | 46.3 | 487 | 9.5 | 475 | 6.4 |
| 20-1-14 | 62 | 54 | 767 | 0.07 | 0.0582 | 0.0012 | 0.6119 | 0.0133 | 0.0760 | 0.0009 | 600 | 44.4 | 485 | 8.4 | 472 | 5.3 |
| 20-1-15 | 76 | 138 | 479 | 0.29 | 0.0585 | 0.0013 | 0.6026 | 0.0136 | 0.0747 | 0.0008 | 550 | 50.0 | 479 | 8.6 | 464 | 4.8 |
| 20-1-16 | 51 | 46 | 544 | 0.09 | 0.0552 | 0.0011 | 0.6034 | 0.0136 | 0.0791 | 0.0010 | 417 | 46.3 | 479 | 8.6 | 491 | 6.0 |
| 20-1-19 | 109 | 172 | 808 | 0.21 | 0.0573 | 0.0013 | 0.6070 | 0.0142 | 0.0763 | 0.0010 | 502 | 48.1 | 482 | 9.0 | 474 | 6.3 |
| 20-1-23 | 85 | 68 | 1064 | 0.06 | 0.0574 | 0.0009 | 0.6188 | 0.0109 | 0.0781 | 0.0009 | 506 | 32.4 | 489 | 6.8 | 485 | 5.6 |
| 20-1-32 | 69 | 65 | 771 | 0.08 | 0.0556 | 0.0011 | 0.5826 | 0.0121 | 0.0757 | 0.0008 | 439 | 42.6 | 466 | 7.8 | 470 | 5.1 |
| 20-1-33 | 116 | 157 | 1054 | 0.15 | 0.0556 | 0.0010 | 0.5946 | 0.0122 | 0.0771 | 0.0010 | 439 | 38.9 | 474 | 7.8 | 479 | 6.1 |
| 20-1-34 | 54 | 40 | 662 | 0.06 | 0.0572 | 0.0012 | 0.6060 | 0.0133 | 0.0765 | 0.0011 | 498 | 46.3 | 481 | 8.4 | 475 | 6.4 |
| 20-1-35 | 52 | 49 | 608 | 0.08 | 0.0558 | 0.0011 | 0.5982 | 0.0114 | 0.0774 | 0.0008 | 456 | 10.2 | 476 | 7.3 | 480 | 4.9 |
| 28-2 花岗质片麻岩 | | | | | | | | | | | | | | | | |
| 28-2-01 | 136 | 304 | 568 | 0.53 | 0.0554 | 0.0011 | 0.6329 | 0.0127 | 0.0827 | 0.0009 | 428 | 42.6 | 498 | 7.9 | 512 | 5.1 |
| 28-2-02 | 239 | 593 | 797 | 0.74 | 0.0563 | 0.0011 | 0.5980 | 0.0115 | 0.0770 | 0.0007 | 465 | 42.6 | 476 | 7.3 | 478 | 4.3 |
| 28-2-04 | 73 | 164 | 254 | 0.65 | 0.0591 | 0.0023 | 0.6192 | 0.0269 | 0.0757 | 0.0012 | 569 | 87.0 | 489 | 16.8 | 470 | 7.3 |
| 28-2-05 | 96 | 216 | 399 | 0.54 | 0.0550 | 0.0013 | 0.5932 | 0.0145 | 0.0783 | 0.0008 | 409 | 49.1 | 473 | 9.3 | 486 | 4.7 |
| 28-2-09 | 88 | 197 | 420 | 0.47 | 0.0581 | 0.0014 | 0.6157 | 0.0139 | 0.0771 | 0.0008 | 532 | 51.8 | 487 | 8.8 | 479 | 4.6 |
| 28-2-10 | 93 | 223 | 384 | 0.58 | 0.0544 | 0.0014 | 0.5810 | 0.0153 | 0.0773 | 0.0008 | 387 | 57.4 | 465 | 9.8 | 480 | 4.9 |
| 28-2-11 | 116 | 260 | 520 | 0.50 | 0.0557 | 0.0012 | 0.6087 | 0.0134 | 0.0793 | 0.0008 | 443 | 54.6 | 483 | 8.5 | 492 | 5.0 |
| 28-2-12 | 103 | 238 | 375 | 0.64 | 0.0578 | 0.0020 | 0.5984 | 0.0212 | 0.0758 | 0.0012 | 520 | 75.9 | 476 | 13.5 | 471 | 6.9 |
| 28-2-14 | 114 | 262 | 408 | 0.64 | 0.0593 | 0.0020 | 0.6322 | 0.0229 | 0.0766 | 0.0012 | 589 | 72.2 | 497 | 14.2 | 476 | 7.2 |
| 28-2-15 | 89 | 187 | 376 | 0.50 | 0.0551 | 0.0017 | 0.6155 | 0.0195 | 0.0813 | 0.0010 | 417 | 70.4 | 487 | 12.3 | 504 | 6.0 |
| 28-2-16 | 86 | 201 | 312 | 0.64 | 0.0555 | 0.0022 | 0.5777 | 0.0227 | 0.0760 | 0.0010 | 432 | 88.9 | 463 | 14.6 | 472 | 5.9 |
| 28-2-17 | 106 | 203 | 532 | 0.38 | 0.0587 | 0.0018 | 0.6163 | 0.0175 | 0.0767 | 0.0010 | 554 | 66.7 | 488 | 11.0 | 477 | 5.9 |
| 28-2-18 | 381 | 977 | 1092 | 0.90 | 0.0561 | 0.0012 | 0.5896 | 0.0121 | 0.0761 | 0.0008 | 457 | 46.3 | 471 | 7.8 | 473 | 4.8 |
| 34-1 花岗质片麻岩 | | | | | | | | | | | | | | | | |
| 34-1-01 | 923 | 1960 | 3298 | 0.59 | 0.0568 | 0.0007 | 0.5813 | 0.0081 | 0.0737 | 0.0005 | 483 | 32.4 | 465 | 5.2 | 459 | 3.2 |
| 34-1-02 | 361 | 671 | 1546 | 0.43 | 0.0570 | 0.0009 | 0.5888 | 0.0099 | 0.0745 | 0.0007 | 494 | 35.2 | 470 | 6.3 | 463 | 4.0 |
| 34-1-03 | 1058 | 2114 | 2699 | 0.78 | 0.0565 | 0.0007 | 0.6336 | 0.0092 | 0.0809 | 0.0007 | 472 | 23.1 | 498 | 5.7 | 501 | 4.2 |
| 34-1-06 | 459 | 875 | 1898 | 0.46 | 0.0567 | 0.0009 | 0.5740 | 0.0093 | 0.0731 | 0.0006 | 480 | 39.8 | 461 | 6.0 | 455 | 3.6 |
| 34-1-07 | 333 | 597 | 1310 | 0.46 | 0.0562 | 0.0010 | 0.5908 | 0.0106 | 0.0764 | 0.0007 | 461 | 38.9 | 471 | 6.8 | 474 | 4.2 |
| 34-1-08 | 413 | 820 | 1403 | 0.58 | 0.0554 | 0.0008 | 0.5744 | 0.0088 | 0.0749 | 0.0005 | 428 | 33.3 | 461 | 5.7 | 466 | 3.2 |
| 34-1-12 | 349 | 647 | 1318 | 0.49 | 0.0570 | 0.0009 | 0.6035 | 0.0098 | 0.0764 | 0.0006 | 500 | 33.3 | 479 | 6.2 | 475 | 3.6 |
| 34-1-13 | 475 | 857 | 1602 | 0.54 | 0.0567 | 0.0009 | 0.6220 | 0.0105 | 0.0793 | 0.0008 | 480 | 39.8 | 491 | 6.6 | 492 | 4.6 |
| 34-1-14 | 583 | 1047 | 2218 | 0.47 | 0.0567 | 0.0008 | 0.6259 | 0.0111 | 0.0796 | 0.0009 | 480 | 36.1 | 494 | 7.0 | 494 | 5.2 |
| 34-1-15 | 1006 | 2141 | 3525 | 0.61 | 0.0566 | 0.0007 | 0.5798 | 0.0075 | 0.0741 | 0.0005 | 476 | 25.9 | 464 | 4.8 | 461 | 3.3 |
| 34-1-16 | 797 | 1760 | 2481 | 0.71 | 0.0566 | 0.0007 | 0.5938 | 0.0082 | 0.0759 | 0.0005 | 476 | 25.0 | 473 | 5.2 | 471 | 3.2 |
| 34-1-18 | 572 | 1091 | 2081 | 0.52 | 0.0570 | 0.0009 | 0.6034 | 0.0100 | 0.0766 | 0.0006 | 500 | 33.3 | 479 | 6.3 | 476 | 3.7 |
| 34-1-19 | 396 | 782 | 1199 | 0.65 | 0.0568 | 0.0009 | 0.6158 | 0.0114 | 0.0784 | 0.0008 | 483 | 32.4 | 487 | 7.2 | 487 | 5.0 |

表3　亚东地区早古生代花岗质片麻岩锆石稀土元素分析表（×10⁻⁶）

Table 3　Zircon REE data of the Early Paleozoic granitic gneisses from the Yadong（×10⁻⁶）

| Spot No. | La | Ce | Pr | Nd | Sm | Eu | Gd | Tb | Dy | Ho | Er | Tm | Yb | Lu | ΣREE | δEu |
|---|---|---|---|---|---|---|---|---|---|---|---|---|---|---|---|---|
| 20-1 | | | | | | | | | | | | | | | | |
| 20-1-02 | bd | 0.60 | 0.024 | 0.52 | 3.07 | 0.040 | 31.7 | 15.36 | 219 | 81.6 | 380 | 76.3 | 762 | 131 | 1701 | 0.18 |
| 20-1-04 | 0.001 | 1.03 | 0.039 | 0.97 | 3.64 | 0.136 | 31.0 | 15.08 | 203 | 74.5 | 353 | 70.7 | 718 | 121 | 1592 | 0.19 |
| 20-1-06 | 0.028 | 0.71 | 0.067 | 1.18 | 3.93 | 0.116 | 42.2 | 23.10 | 337 | 127.5 | 627 | 131.7 | 1392 | 234 | 2921 | 0.19 |
| 20-1-09 | 0.009 | 0.45 | 0.019 | 0.04 | 1.75 | 0.076 | 20.0 | 10.76 | 169 | 66.5 | 327 | 68.5 | 690 | 120 | 1474 | 0.19 |
| 20-1-12 | 0.217 | 1.76 | 0.091 | 1.02 | 3.27 | 0.094 | 29.7 | 14.62 | 213 | 80.8 | 383 | 77.9 | 786 | 134 | 1725 | 0.18 |
| 20-1-14 | 0.0598 | 0.50 | 0.005 | 0.52 | 2.46 | 0.029 | 23.0 | 12.46 | 175 | 65.9 | 302 | 61.4 | 617 | 105 | 1365 | 0.20 |
| 20-1-15 | bd | 1.61 | 0.043 | 1.05 | 3.20 | 0.072 | 25.1 | 10.11 | 142 | 53.9 | 255 | 52.6 | 543 | 98 | 1185 | 0.17 |
| 20-1-16 | bd | 0.51 | 0.017 | 0.58 | 1.54 | 0.038 | 18.7 | 9.30 | 139 | 53.6 | 265 | 55.7 | 562 | 97 | 1203 | 0.18 |
| 20-1-19 | 0.063 | 3.20 | 0.035 | 1.11 | 4.13 | 0.172 | 34.8 | 17.55 | 250 | 98.4 | 461 | 92.6 | 922 | 157 | 2042 | 0.19 |
| 20-1-23 | bd | 0.51 | 0.029 | 0.71 | 3.12 | 0.088 | 31.3 | 15.89 | 236 | 86.1 | 399 | 80.0 | 803 | 137 | 1793 | 0.19 |
| 20-1-32 | 0.077 | 0.74 | 0.030 | 0.43 | 2.61 | 0.153 | 27.9 | 15.07 | 216 | 81.0 | 374 | 75.1 | 758 | 131 | 1682 | 0.19 |
| 20-1-33 | 0.423 | 2.62 | 0.224 | 2.44 | 5.39 | bd | 45.8 | 22.57 | 313 | 114.2 | 517 | 103.7 | 1029 | 172 | 2328 | 0.19 |
| 20-1-34 | bd | 0.38 | 0.013 | 0.29 | 1.74 | 0.018 | 23.6 | 11.53 | 155 | 50.7 | 223 | 45.3 | 452 | 78 | 1043 | 0.19 |
| 20-1-35 | 0.008 | 0.41 | 0.032 | 0.23 | 2.18 | 0.105 | 25.1 | 12.56 | 168 | 61.2 | 276 | 55.8 | 554 | 96 | 1252 | 0.19 |
| 28-2 | | | | | | | | | | | | | | | | |
| 28-2-01 | 0.023 | 18.58 | 0.080 | 1.56 | 4.68 | 0.863 | 31.4 | 12.84 | 180 | 72.1 | 353 | 77.2 | 816 | 144 | 1712 | 0.17 |
| 28-2-02 | bd | 33.02 | 0.053 | 1.96 | 4.46 | 1.061 | 32.5 | 12.65 | 174 | 68.8 | 345 | 76.3 | 818 | 144 | 1713 | 0.17 |
| 28-2-04 | 0.034 | 12.98 | 0.096 | 1.57 | 3.51 | 0.734 | 20.6 | 7.14 | 97 | 37.6 | 184 | 42.2 | 478 | 82 | 968 | 0.16 |
| 28-2-05 | 0.001 | 13.47 | 0.049 | 0.96 | 2.57 | 0.431 | 17.6 | 6.85 | 96 | 37.5 | 185 | 40.3 | 440 | 77 | 918 | 0.17 |
| 28-2-09 | 0.064 | 13.36 | 0.038 | 1.23 | 2.20 | 0.814 | 22.3 | 8.37 | 116 | 45.7 | 236 | 53.6 | 603 | 109 | 1211 | 0.17 |
| 28-2-10 | bd | 10.24 | 0.118 | 1.74 | 4.15 | 0.957 | 30.3 | 11.19 | 154 | 59.0 | 287 | 63.5 | 678 | 119 | 1420 | 0.16 |
| 28-2-11 | 0.060 | 16.34 | 0.116 | 1.48 | 4.43 | 1.166 | 33.2 | 13.94 | 202 | 80.5 | 399 | 88.0 | 962 | 158 | 1960 | 0.17 |
| 28-2-12 | 0.413 | 13.96 | 0.200 | 2.45 | 4.05 | 0.948 | 22.3 | 7.95 | 108 | 39.9 | 201 | 47.1 | 516 | 87 | 1051 | 0.16 |
| 28-2-14 | 0.916 | 19.91 | 0.356 | 2.29 | 3.34 | 0.692 | 18.2 | 7.22 | 104 | 39.5 | 196 | 45.0 | 488 | 80 | 1006 | 0.17 |
| 28-2-15 | bd | 11.71 | 0.058 | 1.09 | 3.57 | 1.025 | 24.0 | 10.07 | 144 | 57.7 | 288 | 64.6 | 708 | 116 | 1430 | 0.17 |
| 28-2-16 | 0.073 | 14.24 | 0.000 | 0.59 | 1.96 | 0.459 | 12.7 | 5.08 | 68 | 28.3 | 141 | 33.3 | 377 | 63 | 744 | 0.17 |
| 28-2-17 | bd | 17.46 | 0.080 | 0.72 | 2.30 | 0.981 | 29.0 | 11.45 | 165 | 66.2 | 326 | 75.6 | 855 | 131 | 1680 | 0.17 |
| 28-2-18 | bd | 35.48 | 0.178 | 1.90 | 5.42 | 1.168 | 34.0 | 12.67 | 165 | 62.8 | 311 | 72.5 | 802 | 133 | 1637 | 0.17 |
| 34-1 | | | | | | | | | | | | | | | | |
| 34-1-01 | bd | 28.24 | 0.080 | 2.04 | 7.42 | 1.012 | 61.3 | 24.56 | 326 | 129.7 | 606 | 127.9 | 1247 | 217 | 2779 | 0.17 |
| 34-1-02 | 0.062 | 25.08 | 0.070 | 1.28 | 5.05 | 0.715 | 33.7 | 13.82 | 188 | 76.0 | 370 | 80.9 | 823 | 146 | 1765 | 0.17 |
| 34-1-03 | 0.652 | 41.61 | 0.463 | 5.17 | 9.06 | 1.332 | 68.5 | 25.45 | 335 | 125.9 | 577 | 119.5 | 1151 | 199 | 2659 | 0.17 |
| 34-1-06 | 0.018 | 24.11 | 0.106 | 1.88 | 5.56 | 0.826 | 46.8 | 18.56 | 246 | 98.8 | 464 | 100.0 | 1011 | 177 | 2196 | 0.17 |
| 34-1-07 | 0.005 | 27.76 | 0.082 | 1.78 | 5.27 | 0.870 | 44.1 | 17.45 | 230 | 92.7 | 434 | 92.4 | 928 | 163 | 2037 | 0.17 |
| 34-1-08 | 0.025 | 26.63 | 0.039 | 2.21 | 5.51 | 0.861 | 38.5 | 14.97 | 201 | 79.4 | 371 | 78.2 | 772 | 136 | 1726 | 0.17 |
| 34-1-12 | 0.647 | 28.95 | 1.018 | 8.80 | 8.24 | 0.906 | 43.0 | 16.11 | 212 | 82.5 | 389 | 83.6 | 824 | 145 | 1844 | 0.17 |
| 34-1-13 | bd | 24.58 | 0.074 | 1.90 | 5.28 | 0.793 | 37.5 | 14.44 | 192 | 75.6 | 355 | 75.5 | 751 | 133 | 1665 | 0.17 |
| 34-1-14 | bd | 27.37 | 0.070 | 1.50 | 5.46 | 0.884 | 45.9 | 18.71 | 249 | 100.1 | 470 | 100.7 | 1000 | 176 | 2195 | 0.18 |
| 34-1-15 | 0.003 | 28.20 | 0.086 | 2.09 | 6.56 | 0.998 | 63.2 | 26.16 | 350 | 136.2 | 633 | 132.7 | 1298 | 224 | 2901 | 0.18 |
| 34-1-16 | 0.139 | 43.38 | 0.153 | 2.83 | 8.78 | 1.150 | 69.5 | 26.13 | 339 | 129.6 | 598 | 125.6 | 1226 | 210 | 2781 | 0.17 |
| 34-1-18 | bd | 23.44 | 0.062 | 1.07 | 4.77 | 0.689 | 39.2 | 15.84 | 213 | 85.3 | 401 | 85.6 | 846 | 150 | 1867 | 0.17 |
| 34-1-19 | bd | 25.50 | 0.050 | 2.16 | 5.48 | 0.911 | 39.2 | 15.17 | 205 | 80.6 | 378 | 80.4 | 795 | 139 | 1766 | 0.17 |

注：bd 代表低于检测下限
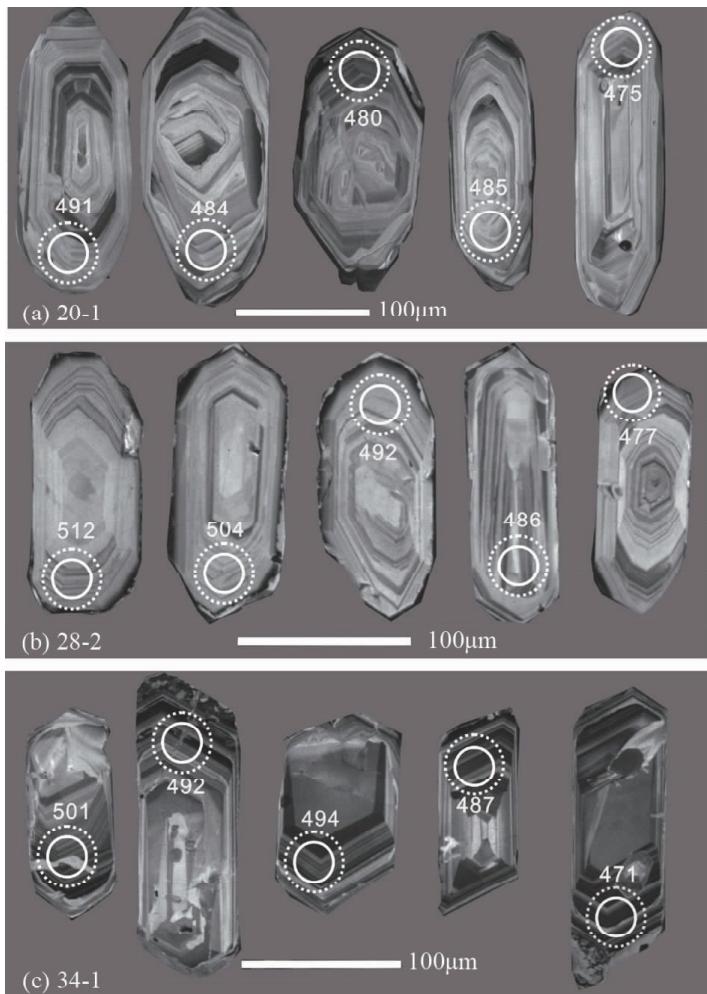
图 5　典型锆石阴极发光图像

实线圆圈为 U-Pb 年龄分析点,虚线圆圈为 Hf 同位素分析点

Fig. 5　Cathodoluminescence images of zircons

The actual line circles and dotted line circles indicate the locations of U-Pb dating and Hf isotopic analyses, respectively

析点的年龄变年轻(Geisler et al. , 2007),其 Th/U 比值也会变小(表2)。因此,所获得的最大年龄,即 491Ma、512Ma 和 501Ma 很可能代表三个花岗质片麻岩样品的原岩结晶年龄。大多数变质增生边较窄,无法进行定年分析。少数较宽的变质增生边获得了约 25Ma 的谐和年龄,表明花岗质片麻岩经历了新生代变质作用。

### 5.2　Hf 同位素特征

对 3 个样品中锆石的岩浆核进行了原位 Hf 同位素分析(表4)。其中样品 20-1 的 14 个分析点获得的$(^{176}Hf/^{177}Hf)_i$值为 0.282248 ~ 0.282480,$\varepsilon_{Hf}(t)$为 − 8.1 ~ + 0.1(图7),相对应的 Hf 二阶段模式年龄($t_{DM2}$)为 1440 ~ 1959Ma。样品 28-2 的 13 个分析点获得的$(^{176}Hf/^{177}Hf)_i$值为 0.282305 ~ 0.282413,$\varepsilon_{Hf}(t)$为 − 5.9 ~ − 2.1(图7),相对应的$t_{DM2}$为 1585 ~ 1826Ma。样品 34-1 的 13 个分析点获得的$(^{176}Hf/^{177}Hf)_i$值为 0.282333 ~ 0.282661,$\varepsilon_{Hf}(t)$为 − 4.8 ~ + 6.7(图7),对应的$t_{DM2}$为 1028 ~ 1762Ma(表4)。

## 6　讨论与结论

### 6.1　喜马拉雅带的早古生代岩浆作用

较早期的研究表明,亚东地区的矽线石榴黑云斜长片麻岩是早古生代(512Ma)花岗岩变质作用的产物(许志琴等,2005)。后来的研究也表明,亚东地区花岗质片麻岩的原岩年龄约为 500Ma(Liu et al. , 2006;时超等,2010)。本研究进一步证明亚东地区花岗质片麻岩的原岩年龄为 491 ~ 512Ma。这些结果都表明,亚东地区广泛发育早古生代的花岗岩。

近年来的研究表明,喜马拉雅岩系中普遍存在早古生代的岩浆岩。如尼泊尔高喜马拉雅岩系中的花岗片麻岩的原岩年龄为 470 ~ 502Ma(Godin et al. , 2001;Johnson et al. , 2001;Gehrels et al. , 2003;Cawood and Buchan, 2007)。印度北部高喜马拉雅岩系中也报道了约 500Ma 的花岗片麻岩(Jäger et al. , 1971;Miller et al. , 2001;Spencer et al. , 2012)。喜马拉雅东构造结高喜马拉雅结晶岩系中的正片麻岩的原岩年龄为 490 ~ 500Ma(张泽明等,2008,2013)。西藏吉隆高喜马拉雅岩系中的二云二长片麻岩的原岩年龄为 474 ~ 514Ma(许志琴等,2005;王晓先等,2011;Wang et al. , 2012a;蔡志慧等,2013)。在特提斯喜马拉雅岩系的片麻岩穹窿中也普遍存在原岩为早古生代的花岗质片麻岩。如康马穹窿中的花岗质片麻岩的原岩年龄为 495 ~ 515Ma(Lee et al. , 2000;Wang et al. , 2012a),雅拉香波穹窿中的花岗片麻岩的原岩年龄为 488 ~ 496Ma(Zeng et al. , 2011;Wang et al. , 2012a;Gao and Zeng, 2014),拉轨岗日穹窿中的花岗片麻岩的原岩年龄为 514Ma(辜平阳等,2013)。这些研究表明,印度大陆北缘经历了强烈的早古生代岩浆作用。

### 6.2　岩石成因

岩石化学分析结果表明,所研究的早古生代花岗岩可分为两类,第一类的 $Na_2O$ 含量 < 3%,$K_2O/Na_2O > 1$,A/CNK > 1.1;第二类的 $Na_2O$ 含量 > 3%,$K_2O/Na_2O < 1$,A/CNK < 1.1(表1和图3)。前者显示 S 型花岗岩的成分特征,后者显示 I 型花岗岩的成分特征(Chappell and White, 1974, 1992)。第一类 S 型花岗岩的岩浆锆石具有显著的 Eu 负异常(表3、图6),为 S 型花岗岩中锆石的典型特征(Wang et al. , 2012b)。S 型花岗岩中的锆石具有较低的$^{176}Hf/^{177}Hf$ 初始比值和负的 $\varepsilon_{Hf}(t)$ 值,对应的 Hf 二阶段模式年龄为 1440 ~ 1959Ma(图7、表4),表明它源于古老变质沉积岩的部分熔融。一个 I 型花岗岩中的锆石具有较分散的 $\varepsilon_{Hf}(t)$ 值( − 4.8 ~ + 6.7),但大多数为正值,相应的 Hf 二阶段模式年龄为 1028 ~ 1762Ma(图7、表4),这很可能表明它是早古生代初生地壳部分熔融的产物,但受到了源于古老表壳岩部分熔融形成的熔体的混染(Liu et al. , 2009;Gagnevin et al. , 2011)。

表4 亚东早古生代花岗质片麻岩中的锆石 Lu-Hf 同位素组成

Table 4   Lu-Hf isotopic data of zircon grains of Early Paleozoic granitic gneisses from Yadong

| Spot No. | Age(Ma) | $^{176}$Hf/$^{177}$Hf | $1\sigma$ | $^{176}$Lu/$^{177}$Hf | $1\sigma$ | $^{176}$Yb/$^{177}$Hf | $1\sigma$ | $(^{176}$Hf/$^{177}$Hf$)_i$ | $\varepsilon_{Hf}(t)$ | $1\sigma$ | $t_{DM}$(Ma) | $t_{DM2}$(Ma) | $f_{Lu/Hf}$ |
|---|---|---|---|---|---|---|---|---|---|---|---|---|---|
| 20-1 | | | | | | | | | | | | | |
| 20-1-02 | | 0.282455 | 0.000027 | 0.001610 | 0.000007 | 0.064848 | 0.000356 | 0.282440 | −1.3 | 1.0 | 1145 | 1529 | −0.95 |
| 20-1-04 | | 0.282305 | 0.000021 | 0.001602 | 0.000016 | 0.054211 | 0.000647 | 0.282291 | −6.6 | 0.7 | 1358 | 1863 | −0.95 |
| 20-1-06 | | 0.282400 | 0.000025 | 0.003115 | 0.000021 | 0.129912 | 0.001299 | 0.282373 | −3.7 | 0.9 | 1274 | 1680 | −0.91 |
| 20-1-09 | | 0.282409 | 0.000025 | 0.001645 | 0.000016 | 0.067686 | 0.000632 | 0.282394 | −2.9 | 0.9 | 1212 | 1632 | −0.95 |
| 20-1-12 | | 0.282342 | 0.000026 | 0.001225 | 0.000012 | 0.050776 | 0.000553 | 0.282331 | −5.1 | 0.9 | 1292 | 1773 | −0.96 |
| 20-1-14 | | 0.282402 | 0.000023 | 0.001322 | 0.000007 | 0.052439 | 0.000358 | 0.282390 | −3.0 | 0.8 | 1211 | 1641 | −0.96 |
| 20-1-15 | | 0.282265 | 0.000026 | 0.001214 | 0.000028 | 0.046353 | 0.001020 | 0.282254 | −7.9 | 0.9 | 1400 | 1946 | −0.96 |
| 20-1-16 | 491 | 0.282494 | 0.000017 | 0.001509 | 0.000011 | 0.049402 | 0.000340 | 0.282480 | 0.1 | 0.6 | 1087 | 1440 | −0.95 |
| 20-1-19 | | 0.282483 | 0.000030 | 0.002607 | 0.000018 | 0.093840 | 0.000853 | 0.282460 | −0.6 | 1.1 | 1136 | 1486 | −0.92 |
| 20-1-23 | | 0.282389 | 0.000024 | 0.004000 | 0.000042 | 0.135072 | 0.001243 | 0.282353 | −4.4 | 0.9 | 1324 | 1724 | −0.88 |
| 20-1-32 | | 0.282284 | 0.000028 | 0.001761 | 0.000038 | 0.057836 | 0.001748 | 0.282269 | −7.3 | 1.0 | 1393 | 1913 | −0.95 |
| 20-1-33 | | 0.282429 | 0.000030 | 0.003202 | 0.000034 | 0.118398 | 0.001455 | 0.282400 | −2.7 | 1.0 | 1235 | 1618 | −0.90 |
| 20-1-34 | | 0.282328 | 0.000025 | 0.001024 | 0.000044 | 0.038208 | 0.001253 | 0.282319 | −5.6 | 0.9 | 1305 | 1800 | −0.97 |
| 20-1-35 | | 0.282264 | 0.000019 | 0.001823 | 0.000028 | 0.065177 | 0.000942 | 0.282248 | −8.1 | 0.7 | 1424 | 1959 | −0.95 |
| 28-2 | | | | | | | | | | | | | |
| 28-2-01 | | 0.282392 | 0.000041 | 0.005111 | 0.000039 | 0.143468 | 0.000918 | 0.282346 | −4.4 | 1.5 | 1363 | 1735 | −0.85 |
| 28-2-02 | | 0.282323 | 0.000035 | 0.001976 | 0.000013 | 0.056384 | 0.000347 | 0.282305 | −5.9 | 1.2 | 1346 | 1826 | −0.94 |
| 28-2-04 | | 0.282391 | 0.000019 | 0.002755 | 0.000017 | 0.106257 | 0.000632 | 0.282366 | −3.7 | 0.7 | 1276 | 1691 | −0.92 |
| 28-2-05 | | 0.282343 | 0.000033 | 0.003646 | 0.000076 | 0.103863 | 0.002347 | 0.282310 | −5.7 | 1.2 | 1380 | 1816 | −0.89 |
| 28-2-09 | | 0.282427 | 0.000030 | 0.002000 | 0.000010 | 0.054426 | 0.000259 | 0.282409 | −2.2 | 1.1 | 1197 | 1594 | −0.94 |
| 28-2-10 | | 0.282399 | 0.000021 | 0.002244 | 0.000028 | 0.081480 | 0.001480 | 0.282379 | −3.3 | 0.7 | 1245 | 1661 | −0.93 |
| 28-2-11 | 512 | 0.282436 | 0.000044 | 0.002568 | 0.000038 | 0.066077 | 0.001000 | 0.282413 | −2.1 | 1.6 | 1203 | 1585 | −0.92 |
| 28-2-12 | | 0.282423 | 0.000029 | 0.002876 | 0.000028 | 0.079778 | 0.000563 | 0.282397 | −2.6 | 1.0 | 1233 | 1621 | −0.91 |
| 28-2-14 | | 0.282399 | 0.000019 | 0.002498 | 0.000021 | 0.100079 | 0.000920 | 0.282376 | −3.4 | 0.7 | 1255 | 1668 | −0.92 |
| 28-2-15 | | 0.282411 | 0.000023 | 0.002245 | 0.000007 | 0.062844 | 0.000776 | 0.282391 | −2.9 | 0.8 | 1229 | 1635 | −0.93 |
| 28-2-16 | | 0.282396 | 0.000020 | 0.002003 | 0.000021 | 0.076029 | 0.001000 | 0.282378 | −3.3 | 0.7 | 1243 | 1664 | −0.94 |
| 28-2-17 | | 0.282424 | 0.000029 | 0.003218 | 0.000033 | 0.079800 | 0.000607 | 0.282395 | −2.7 | 1.0 | 1243 | 1625 | −0.90 |
| 28-2-18 | | 0.282382 | 0.000026 | 0.002115 | 0.000046 | 0.060990 | 0.001543 | 0.282363 | −3.8 | 0.9 | 1266 | 1697 | −0.94 |
| 34-1 | | | | | | | | | | | | | |
| 34-1-01 | | 0.282565 | 0.000026 | 0.001214 | 0.000028 | 0.046353 | 0.001020 | 0.282554 | 3.0 | 0.9 | 978 | 1268 | −0.96 |
| 34-1-02 | | 0.282675 | 0.000023 | 0.001635 | 0.000037 | 0.058568 | 0.001205 | 0.282661 | 6.7 | 0.8 | 831 | 1028 | −0.95 |
| 34-1-03 | | 0.282618 | 0.000032 | 0.003733 | 0.000053 | 0.146356 | 0.001303 | 0.282584 | 4.0 | 1.1 | 968 | 1201 | −0.89 |
| 34-1-06 | | 0.282643 | 0.000025 | 0.002748 | 0.000017 | 0.125429 | 0.000508 | 0.282618 | 5.2 | 0.9 | 904 | 1124 | −0.92 |
| 34-1-07 | | 0.282491 | 0.000034 | 0.003086 | 0.000018 | 0.111231 | 0.000406 | 0.282462 | −0.3 | 1.2 | 1140 | 1473 | −0.91 |
| 34-1-08 | | 0.282621 | 0.000023 | 0.002269 | 0.000007 | 0.085080 | 0.000393 | 0.282600 | 4.6 | 0.8 | 925 | 1164 | −0.93 |
| 34-1-12 | 501 | 0.282523 | 0.000023 | 0.002327 | 0.000016 | 0.094659 | 0.000709 | 0.282502 | 1.1 | 0.8 | 1068 | 1384 | −0.93 |
| 34-1-13 | | 0.282459 | 0.000023 | 0.002828 | 0.000009 | 0.117244 | 0.000354 | 0.282433 | −1.3 | 0.8 | 1178 | 1539 | −0.91 |
| 34-1-14 | | 0.282371 | 0.000038 | 0.004189 | 0.000042 | 0.155850 | 0.001620 | 0.282333 | −4.8 | 1.4 | 1358 | 1762 | −0.87 |
| 34-1-15 | | 0.282367 | 0.000021 | 0.003493 | 0.000056 | 0.131642 | 0.002070 | 0.282335 | −4.8 | 0.8 | 1338 | 1757 | −0.89 |
| 34-1-16 | | 0.282594 | 0.000021 | 0.002237 | 0.000037 | 0.089818 | 0.000971 | 0.282574 | 3.7 | 0.8 | 963 | 1223 | −0.93 |
| 34-1-18 | | 0.282449 | 0.000022 | 0.002369 | 0.000006 | 0.099504 | 0.000342 | 0.282427 | −1.5 | 0.8 | 1178 | 1553 | −0.93 |
| 34-1-19 | | 0.282535 | 0.000023 | 0.002506 | 0.000034 | 0.104732 | 0.001323 | 0.282512 | 1.5 | 0.8 | 1057 | 1362 | −0.92 |
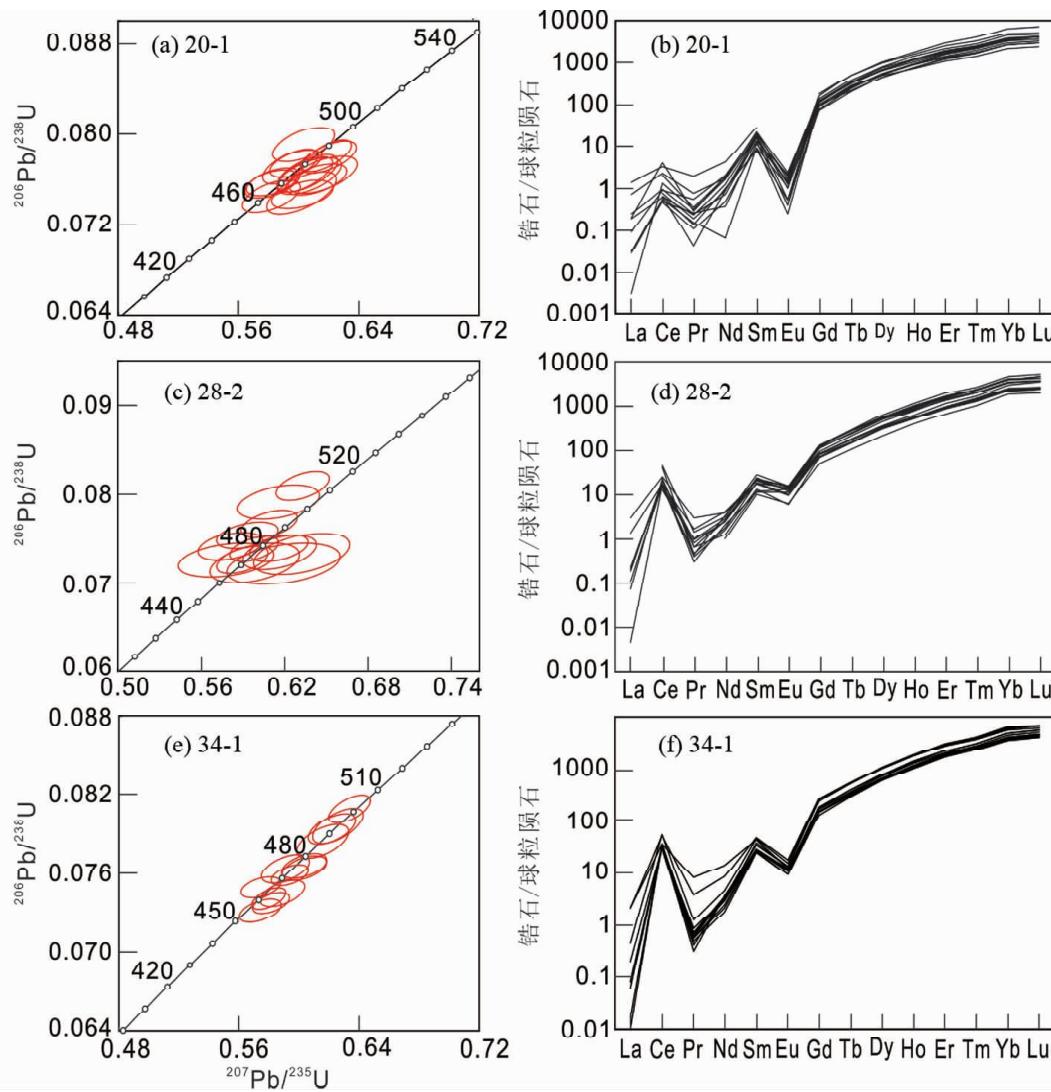
图 6　锆石 U-Pb 谐和曲线和稀土元素配分曲线(球粒陨石标准值据 Taylor and McLennan,1985)

Fig. 6　U-Pb concordia diagrams and chondrite-normalized REE patterns of zircons (chondrite values after Taylor and McLennan, 1985)
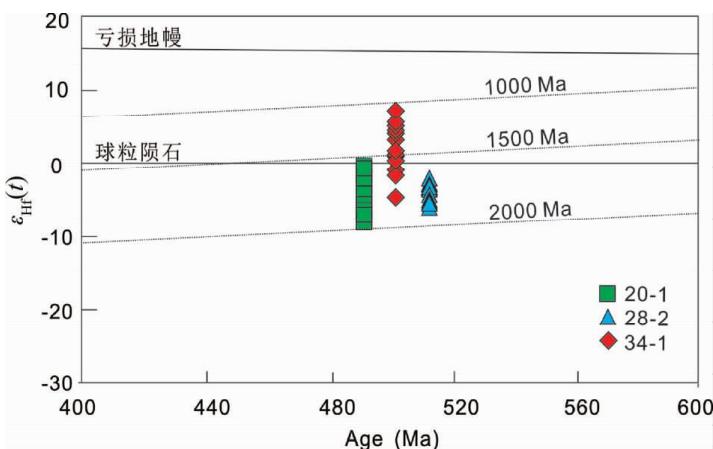


图 7　亚东早古生代花岗质片麻岩的锆石 $\varepsilon_{Hf}(t)$ 与 U-Pb 年龄图

Fig. 7　Plots of $\varepsilon_{Hf}(t)$ vs. zircon U-Pb ages of the Early Paleozoic granitic gneisses from the Yadong

另一个 I 型花岗岩的锆石具有相对集中的负的 $\varepsilon_{Hf}(t)$ 值,相应的 Hf 二阶段模式年龄为 1585～1826Ma,很可能是古元古代岩

浆岩部分熔融的产物。近年来在青藏高原喜马拉雅带、拉萨地体和南羌塘地区陆续发现了古元古代(1600～2000Ma)的岩浆岩(Gehrels et al., 2003; Liu et al., 2009; 王晓先等, 2011; Zhang et al., 2014; 彭智敏等, 2014)。这些岩石很可能是青藏高原南部早古生代花岗岩的原岩。

亚东地区的早古生代 I 花岗岩具有较高的稀土含量,其球粒陨石标准化配分模式表现为 LREE 富集和 HREE 亏损,Eu 负异常(图 4a),微量元素原始地幔标准化配分模式均显出 Nb、Ta、P 和 Ti 的负异常(图 4b),指示岩浆弧花岗岩的地球化学特征(Garzanti et al., 1986; Zhang et al., 2013)。在 Pearce et al. (1984)的花岗岩构造环境判别图解上,亚东地区的 I 型花岗岩均落在岛弧花岗岩或岛弧-同碰撞花岗岩区(图 8)。这些都表明亚东地区的 I 型花岗岩形成在岩浆弧构造环境。

### 6.3　构造意义

泛非造山作用是冈瓦纳大陆聚合过程中陆-陆碰撞的结果,主要发生在 520～570Ma(Cawood and Buchan, 2007)。早期研究认为,冈瓦纳大陆北缘的早古生代岩浆岩是泛非造山
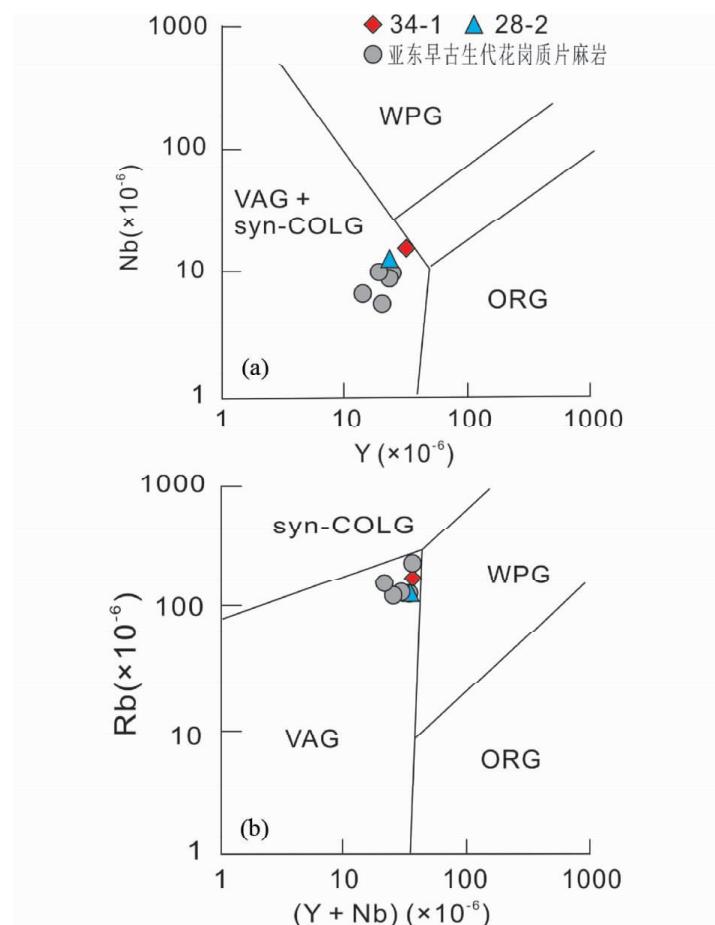
图8 I 型花岗质片麻岩构造环境判别图解(据 Pearce et al. , 1984)

Fig. 8   Diagrams of the tectonic setting for Early Paleozoic I-type granitic gneisses (after Pearce et al. , 1984)

作用的产物,与冈瓦纳大陆聚合有关(McWilliams, 1981;许志琴等,2005;李才等,2010)。然而,越来越多的研究表明,青藏高原南部,包括拉萨地体和羌塘地体中的早古生代岩浆作用发生在 495~515Ma,是冈瓦纳大陆聚合之后的安第斯型造山作用的产物(Gansser, 1964;Collins, 2002;Kusky et al. , 2003;Cawood et al. , 2007;张泽明等,2013;王晓先等,2011;蔡志慧等,2013;Zhang et al. , 2013)。下列证据进一步表明这套花岗岩形成在安第斯型造山作用过程中:(1)与超大陆汇聚有关的泛非造山作用主要发生在冈瓦纳大陆内部,其边缘并没有受到碰撞造山作用的影响(Cawood et al. , 2007;王晓先等,2011);(2)如上所述,早古生代花岗岩多具有弧岩浆岩的特征;(3)冈瓦纳大陆北缘陆续有早古生代基性岩的报道(Brookfield, 1993;Miller et al. , 2001;Visonà et al. , 2010;潘晓萍等,2012;杨学俊等,2012)。Zhu et al. (2012)在拉萨地体中发现了 490Ma 的起源于亏损地幔的基性火山岩,并认为其形成于俯冲洋壳断离构造环境。

以往的研究认为,青藏高原南部的早古生代岩浆岩大多具有负的锆石 $\varepsilon_{Hf}(t)$ 值(Cawood et al. , 2007;董美玲等, 2012;Wang et al. , 2013;Dong et al. , 2013;辜平阳等,2013;张士贞等,2014),因此,大家都认为它们是古老地壳物质部分熔融的产物。本文第一次报道了早古生代花岗岩具有正的锆

石 $\varepsilon_{Hf}(t)$ 值,它们很可能是早古生代的初生地壳物质部分熔融的产物。

本研究表明,亚东及邻区的早古生代花岗岩包括 I 型和 S 型花岗岩。I 型花岗岩的广泛发育,进一步证明了早古生代花岗岩为安第斯造山作用的产物。而且,I 型和 S 型花岗岩的同时存在也被认为是增生造山作用的重要标志(Chappell and White, 1992;Collins, 2002;Kemp et al. , 2009;Zhang et al. , 2013)。

## References

Brookfield ME. 1993. The Himalayan passive margin from Precambrian to Cretaceous. Sedimentary Geology, 84(1-4): 1-35

Cai ZH, Xu ZQ, Duan XD, Li HQ, Cao H and Huang XM. 2013. Early stage of Early Paleozoic orogenic event in western Yunnan Province, southeastern margin of Tibet Plateau. Acta Petrologica Sinica, 29(6): 2123-2140 (in Chinese with English abstract)

Cawood PA and Buchan C. 2007. Linking accretionary orogenesis with supercontinent assembly. Earth-Science Review, 82(3-4): 217-256

Cawood PA, Johnson MRW and Nernch AA. 2007. Early Paleozoic orogenesis along the Indian margin of Gondwana: Tectonic response to Gondwana assembly. Earth and Planetary Science Letters, 255(1-2): 70-84

Chappell BW and White AJR. 1974. Two contrasting granite types. Pacific Geology, 8(1): 173-174

Chappell BW and White AJR. 1992. I- and S-type granites in the Lachlan Fold Belt. Transactions of the Royal Society of Edinburgh: Earth Sciences, 83(1-2): 1-26

Collins WL. 2002. Hot orogens, tectonic switching, and creation of continental crust. Geology, 30(6): 535-538

DeCelles PG, Robison DM, Quade J, Ojha TP, Garzione CN, Gopel P and Upreti BN. 2001. Stratigraphy, structure, and tectonic evolution of the Himalayan fold-thrust belt in western Nepal. Tectonics, 20(4): 487-509

Ding HX, Zhang ZM, Dong X, Yan R, Lin YH and Jiang HY. 2015. Cambrian ultrapotassic rhyolites from the Lhasa terrane, south Tibet: Evidence for Andean-type magmatism along the northern active margin of Gondwana. Gondwana Research, 27(4): 1616-1629

Ding L, Zhong DL, Yin A, Kapp P and Harrison TM. 2001. Cenozoic structural and metamorphic evolution of the eastern Himalayan syntaxis (Namche Barwa). Earth and Planetary Science Letters, 192(3): 423-438

Dong ML, Dong GC, Mo XX, Zhu DC, Nie F, Xie XF, Wang X and Hu ZC. 2012. Geochronology and geochemistry of the Early Palaeozoic granitoids in Baoshan block, western Yunnan and their implications. Acta Petrologica Sinica, 28(5): 1453-1464 (in Chinese with English abstract)

Dong ML, Dong GC, Mo XX, Santosh M, Zhu DC, Yu JC, Nie F and Hu ZC. 2013. Geochemistry, zircon U-Pb geochronology and Hf isotopes of granites in the Baoshan Block, western Yunnan: Implications for Early Paleozoic evolution along the Gondwana margin. Lithos, 179: 36-47

Dong X, Zhang ZM, Wang JL, Zhao GC, Liu F, Wang W and Yu F.

2009. Provenance and formation age of the Nyingchi Group in the southern Lhasa terrane, Tibetan Plateau: Petrology and zircon U-Pb geochronology. Acta Petrologica Sinica, 25(7): 1678 – 1694 (in Chinese with English abstract)

Elhlou S, Belousova E, Griffin WL, Pearson NJ and O'Reilly SY. 2006. Trace element and isotopic composition of GJ red zircon standard by laser ablation. Geochimica et Cosmochimica Acta, 70(18): A158

Frost BR, Arculus RJ, Barnes CG, Collins WJ, Ellis DJ and Frost CD. 2001. A geochemical classification of granitic rocks. Journal of Petrology, 42(11): 2033 – 2048

Gagnevin D, Daly JS, Horstwood MSA and Whitehouse MJ. 2011. In-situ zircon U-Pb, oxygen and hafnium isotopic evidence for magma mixing and mantle metasomatism in the Tuscan magmatic province, Italy. Earth and Planetary Science Letters, 305(1 – 2): 45 – 56

Gansser A. 1964. The Geology of the Himalayas. London: Wiley Interscience, 1 – 288

Gao LE and Zeng LS. 2014. Fluxed melting of metapelite and the formation of Miocene high-CaO two-mica granites in the Malashan gneiss dome, southern Tibet. Geochimica et Cosmochimica Acta, 130: 135 – 155

Garzanti E, Casnedi R and Jadoul F. 1986. Sedimentary evidence of a Cambro-Ordovician orogenic event in the northwestern Himalaya. Sedimentary Geology, 48(3 – 4): 237 – 265

Gehrels GE, Decelles PG, Martin A, Ojha TP, Pinhassi G and Upreti BN. 2003. Initiation of the Himalayan orogen as an Early Paleozoic thin-skinned thrust belts. GSA Today, 13(9): 4 – 9

Geisler T, Schaltegger U and Tomaschek F. 2007. Re-equilibration of zircon in aqueous fluids and melts. Elements, 3(1): 43 – 50

Godin L, Parrish RR, Brown RL and Hodges KV. 2001. Crustal thickening leading to exhumation of the Himalayan metamorphic core of central Nepal: Insight from U-Pb geochronology and $^{40}Ar/^{39}Ar$ thermochronology. Tectonics, 20(5): 729 – 747

Gu PY, He SP, Li RS, Shi C, Dong ZC, Zha XF, Wu JL and Wang Y. 2013. Geochemical features and tectonic significance of granitic gneiss of Laguigangri metamorphic core complexes in southern Tibet. Acta Petrologica Sinica, 29(3): 756 – 768 (in Chinese with English abstract)

Guo ZF and Wilson M. 2012. The Himalayan leucogranites: Constraints on the nature of their crustal source region and geodynamic setting. Gondwana Research, 22(2): 360 – 376

He ZY, Zhang ZM, Zong KQ and Dong X. 2013. Paleoproterozoic crustal evolution of the Tarim Craton: Constrained by zircon U-Pb and Hf isotopes of meta-igneous rocks from Korla and Dunhuang. Journal of Asian Earth Sciences, 78: 54 – 70

Hébert R, Bezard R, Guilmette C, Dostal J, Wang CS and Liu ZF. 2012. The Indus-Yarlung Zangbo ophiolites from Nanga Parbat to Namche Barwa syntaxes, southern Tibet: First synthesis of petrology, geochemistry, and geochronology with incidences on geodynamic reconstructions of Neo-Tethys. Gondwana Research, 22(2): 377 – 397

Hoskin PWO and Schaltegger U. 2003. The composition of zircon and igneous and metamorphic petrogenesis. Reviews in Mineralogy and Geochemistry, 53(1): 27 – 62

Hou KJ, Li YH, Zou TR et al. 2007. Laser ablation-MC-ICP-MS technique for Hf isotope microanalysis of zircon and its geological applications. Acta Petrologica Sinica, 23(10): 2595 – 2604 (in Chinese with English abstract)

Hou ZQ, Zheng YC, Zeng LS, Gao LE, Huang KX, Li W, Li QY, Fu Q, Liang W and Sun QZ. 2012. Eocene-Oligocene granitoids in southern Tibet: Constraints on crustal anatexis and tectonic evolution of the Himalayan orogen. Earth and Planetary Science Letters, 349(1): 38 – 52

Jäger E, Bhandarai AK and Bhanot VB. 1971. Rb-Sr age-determinations on biotites and whole rock samples from the Mandi and Chor granites, Himachal Pradesh, India. Ecologae Geologica Helvetia, 64(3): 521 – 527

Johnson MRW, Oliver GJH, Parrish RR and Johnson SP. 2001. Synthrusting metamorphism, cooling, and erosion of the Himalayan Kathmandu complex, Nepal. Tectonics, 20(3): 394 – 415

Kemp AIS, Hawkesworth CJ, Collins WJ, Gray CM, Blevin PL and EIMF. 2009. Isotopic evidence for rapid continental growth in an extensional accretionary orogen: The Tasmanides, eastern Australia. Earth and Planetary Science Letters, 284(3 – 4): 455 – 466

Kusky TM, Abdelsalam M, Tucker RD and Stern RJ. 2003. Evolution of the East African and related orogens, and the assembly of the Gondwana. Precambrian Research, 123(2 – 4): 81 – 85

Lee J, Hacker BR, Dinklage WS, Wang Y, Gans P, Calvert A, Wan JL, Chen WJ, Blythe AE and McClelland W. 2000. Evolution of the Kangmar Dome, southern Tibet: Structural, petrologic, and thermochronologic constraints. Tectonics, 19(5): 872 – 895

Li C, Wu YW, Wang M and Yang HT. 2010. Significant progress on Pan-African and Early Paleozoic orogenic events in Qinghai-Tibet Plateau: Discovery of Pan-African orogenic unconformity and Cambrian System in the Gangdise area, Tibet, China. Geological Bulletin of China, 29(12): 1733 – 1736 (in Chinese with English abstract)

Liu S, Hu RZ, Gao S, Feng CX, Huang ZL, Lai SC, Yuan HL, Liu XM, Coulson IM, Feng GY, Wang T and Qi YQ. 2009. U-Pb zircon, geochemical and Sr-Nd-Hf isotopic constraints on the age and origin of Early Paleozoic I-type granite from the Tengchong-Baoshan Block, western Yunnan Province, SW China. Journal of Asian Earth Sciences, 36(2): 168 – 182

Liu WC, Zhou ZH, Zhang XX and Zhao XG. 2006. SHRIMP zircon geochronological constraints on a Pan-African orogeny in the Yadong area, Southern Tibet. Geochimica et Cosmochimica Acta, 70(18): A365

Liu YS, Hu ZC, Zong KQ, Gao CG, Gao S, Xu J and Chen HH. 2010. Reappraisement and refinement of zircon U-Pb isotope and trace element analyses by LA-ICP-MS. Chinese Science Bulletin, 55(15): 1535 – 1546

Ludwig KR. 2003. Isoplot/Ex Version 3.00: A Geochronological Toolkit for Microsoft Excel. Berkeley: Special Publication, No.4. Berkeley Geochronology Center 1 – 73

Maniar PD and Piccoli PM. 1989. Tectonic discrimination of granites. Geological Society of American Bulletin, 101(5): 635 – 643

McWilliams MO. 1981. Palaeomagnetism and Precambrian tectonic evolution of Gondwana. In: Kröner A (ed.). Precambrian Plate Tectonics. Amsterdam: Elsevier, 649 – 687

Miller C, Thöni M, Frank W, Grasemann B, Klötzli U, Guntli P and Draganits E. 2001. The Early Paleozoic magmatic event in the Northwest Himalaya, India: Source, tectonic setting and age of emplacement. Geological Magazine, 138(3): 237 – 251

Mo XX, Niu YL, Dong GC, Zhao ZD, Hou ZQ, Zhou S and Ke S. 2008. Contribution of syncollisional silicic magmatism to continental crust growth: A case study of the Paleogene Linzizong volcanic Succession in southern Tibet. Chemical Geology, 250(1 – 4): 49 – 67

Pan XP, Li RS, Wang C, Yu PS, Gu PY and Zha XF. 2012. Geochemical characteristics of the Cambrian volcanic rocks in Banglecun area on the northern margin of Gangdise, Nyima County, Tibet. Geological Bulletin of China, 31(1): 63 – 74 (in Chinese with English abstract)

Pearce JA, Harris NBW and Tindle AG. 1984. Trace element discrimination diagrams for the tectonic interpretation of granitic rocks. Journal of Petrology, 25(4): 956 – 983

Peng ZM, Geng QR, Wang LQ, Zhang Z, Guan JL, Cong F and Liu SS. 2014. Zircon U-Pb ages and Hf isotopic characteristics of granitic gneiss from Bunsumco, central Qiangtang, Qinghai-Tibet Plateau. Chinese Science Bulletin, 59(26): 2621 – 2629 (in Chinese)

Rowley DB. 1996. Age of initiation of collision between India and Asia: A review of stratigraphic data. Earth and Planetary Science Letters, 145(1 – 4): 1 – 13

Rubatto D and Scambelluri M. 2003. U-Pb dating of magmatic and metamorphic baddeleyite in the Ligurian eclogite (Voltri Massif, Western Apls). Contributions to Mineralogy and Petrology, 146(3): 341 – 355

Shi C, Li RS, He SP, Wang C, Pan SJ, Liu Y and Gu PY. 2010. LA-ICP-MS zircon U-Pb dating for gneissic garnet-bearing biotite granodiorite in the Yadong area, southern Tibet, China and its geological significance. Geological Bulletin of China, 29(12): 1745

─1753 (in Chinese with English abstract)

Spencer CJ, Harris RA and Dorais MJ. 2012. Depositional provenance of the Himalayan metamorphic core of Garhwal region, India: Constrained by U-Pb and Hf isotopes in zircons. Gondwana Research, 22(1): 26 ─35

Sun SS and McDonough WF. 1989. Chemical and isotopic systematics of oceanic basalts: Implications for mantle composition and processes. In: Saunders AD and Norry MJ (eds.). Magmatism in the Ocean Basins. Geological Society, London, Special Publications, 42(1): 313 ─345

Taylor SR and McLennan SM. 1985. The Continental Crust: Its Composition and Evolution. London: Blackwell, 1 ─328

Visonà D, Rubatto D and Villa IM. 2010. The mafic rocks of Shao La (Kharta, S. Tibet): Ordovician basaltic magmatism in the Greater Himalayan Crystallines of central-eastern Himalaya. Journal of Asian Earth Sciences, 38(1 ─2): 14 ─25

Wang Q, Zhu DC, Zhao ZD, Guan Q, Zhang XQ, Sui QL, Hu ZC and Mo XX. 2012b. Magmatic zircons from I-, S- and A-type granitoids in Tibet: Trace element characteristics and their application to detrital zircon provenance study. Journal of Asian Earth Sciences, 53: 59 ─66

Wang XX, Zhang JJ, Yang XY and Zhang B. 2011. Zircon SHRIMP U-Pb ages, Hf isotopic features and their geological significance of the Greater Himalayan Crystalline Complex augen gneiss in Gyirong area, South Tibet. Earth Science Frontiers, 18(2): 127 ─139 (in Chinese with English abstract)

Wang XX, Zhang JJ, Santosh M, Liu J, Yan SY and Guo L. 2012a. Andean-type orogeny in the Himalayas of South Tibet: Implications for Early Paleozoic tectonics along the Indian margin of Gondwana. Lithos, 154(4): 248 ─262

Wang YJ, Xing XW, Peter A, Lai SC, Xia XP, Fan WM, Liu HC and Zhang FF. 2013. Petrogenesis of Early Paleozoic peraluminous granite in the Sibumasu Block of SW Yunnan and diachronous accretionary orogenesis along the northern margin of Gondwana. Lithos, 182 ─183: 67 ─85

Xu ZQ, Yang JS, Liang FH, Qi XX, Liu FL, Zeng LS, Liu DY, Liu HB, Wu CL, Shi RD and Chen SY. 2005. Pan-African and Early Paleozoic orogenic events in the Himalaya terrane: Inference from SHRIMP U-Pb zircon ages. Acta Petrologica Sinica, 21(1): 1 ─12 (in Chinese with English abstract)

Yang XJ, Jia XC, Xiong CL, Bai XZ, Huang BX, Luo G and Yang CB. 2012. LA-ICP-MS zircon U-Pb age of metamorphic basic volcanic rock in Gongyanghe Group of southern Gaoligong Mountain, western Yunnan Province, and its geological significance. Geological Bulletin of China, 31(1): 264 ─276 (in Chinese with English abstract)

Yin A and Harrison TM. 2000. Geologic evolution of the Himalayan-Tibetan orogeny. Annual Review of Earth and Planetary Sciences, 28(1): 211 ─280

Zeng LS, Gao LE, Xie KJ and Zeng LJ. 2011. Mid-Eocene high Sr/Y granites in the Northern Himalayan Gneiss Domes: Melting thickened lower continental crust. Earth and Planetary Science Letters, 303(3 ─4): 251 ─266

Zhang SZ, Li FQ, Li Y, Liu W and Qin YD. 2014. Early Ordovician strongly peraluminous granite in the middle section of the Yarlung Zangbo junction zone and its geological significance. Science China (Earth Sciences), 57(4): 630 ─643

Zhang ZM, Wang JL, Shen K and Shi C. 2008. Paleozoic circum-Gondwana orogens: Petrology and geochronology of the Namche Barwa Complex in the eastern Himalayan syntaxis, Tibet. Acta Petrologica Sinica, 24(7): 1627 ─1637 (in Chinese with English abstract)

Zhang ZM, Dong X, Xiang H, Liou JG and Santosh M. 2013. Building of the deep Gangdese arc, South Tibet: Paleocene plutonism and granulite-facies metamorphism. Journal of Petrology, 54(12): 2547 ─2580

Zhang ZM, Dong X, He ZY and Xiang H. 2013. Indian and Asian continental collision viewed from HP and UHP metamorphic of the Himalayan orogen. Acta Petrologica Sinica, 29(5): 1713 ─1726 (in Chinese with English abstract)

Zhang ZM, Dong X, Santosh M and Zhao GC. 2014. Metamorphism and tectonic evolution of the Lhasa terrane, Central Tibet. Gondwana Research, 25(1): 170 ─189

Zhang ZM, Xiang H, Dong X, Ding HX and He ZY. 2015. Long-lived high-temperature granulite-facies metamorphism in the Eastern Himalayan orogen, south Tibet. Lithos, 212 ─215: 1 ─15

Zhu DC, Zhao ZD, Niu YL, Dilek Y, Wang Q, Ji WH, Dong GC, Sui QL, Liu YS, Yuan HL and Mo XX. 2012. Cambrian bimodal volcanism in the Lhasa Terrane, southern Tibet: Record of an Early Paleozoic Andean-type magmatic arc in the Australian proto-Tethyan margin. Chemical Geology, 328: 290 ─308

## 附中文参考文献

蔡志慧, 许志琴, 段向东, 李化启, 曹汇, 黄学猛. 2013. 青藏高原东南缘滇西早古生代早期造山事件. 岩石学报, 29(6): 2123 ─2140

董美玲, 董国臣, 莫宣学, 朱弟成, 聂飞, 谢许峰, 王霞, 胡兆初. 2012. 滇西保山地块早古生代花岗岩类的年代学地球化学及意义. 岩石学报, 28(5): 1453 ─1464

董昕, 张泽明, 王金丽, 赵国春, 刘峰, 王伟, 于飞. 2009. 青藏高原拉萨地体南部林芝岩群的物质来源与形成年代: 岩石学与锆石U-Pb 年代学. 岩石学报, 25(7): 1678 ─1694

辜平阳, 何世平, 李荣社, 时超, 董增产, 查显锋, 吴继莲, 王轶. 2013. 藏南拉轨岗日变质核杂岩核部花岗质片麻岩的地球化学特征及构造意义. 岩石学报, 29(3): 756 ─768

侯可军, 李延河, 邹天人等. 2007. LA-MC-ICP-MS 锆石 Hf 同位素的分析方法及地质应用. 岩石学报, 23(10): 2595 ─2604

李才, 吴彦旺, 王明, 杨韩涛. 2010. 青藏高原泛非-早古生代造山事件研究重大进展: 冈底斯地区寒武系和泛非造山不整合的发现. 地质通报, 29(12): 1733 ─1736

潘晓萍, 李荣社, 王超, 于浦生, 辜平阳, 查显锋. 2012. 西藏冈底斯北缘尼玛地区帮勒村一带寒武纪火山岩 LA-ICP-MS 锆石 U-Pb 年龄及其地球化学特征. 地质通报, 31(1): 63 ─74

彭智敏, 耿全如, 王立全, 张璋, 关俊雷, 丛峰, 刘书生. 2014. 青藏高原羌塘中部本松错花岗质片麻岩锆石 U-Pb 年龄、Hf 同位素特征及地质意义. 科学通报, 59(26): 2621 ─2629

时超, 李荣社, 何世平, 王超, 潘术娟, 刘银, 辜平阳. 2010. 藏南亚东地区片麻状含石榴子石黑云花岗闪长岩 LA-ICP-MS 锆石 U-Pb 测年及其地质意义. 地质通报, 29(12): 1745 ─1753

王晓先, 张进江, 杨雄英, 张波. 2011. 藏南吉隆地区早古生代大喜马拉雅片麻岩锆石 SHRIMP U-Pb 年龄、Hf 同位素特征及其地质意义. 地学前缘, 18(2): 127 ─139

许志琴, 杨经绥, 梁凤华, 戚学祥, 刘福来, 曾令森, 刘敦一, 刘海兵, 吴才来, 史仁灯, 陈松永. 2005. 喜马拉雅地体的泛非-早古生代造山事件年龄记录. 岩石学报, 21(1): 1 ─12

杨学俊, 贾小川, 熊昌利, 白宪洲, 黄柏鑫, 罗改, 杨朝碧. 2012. 滇西高黎贡山南段公养河群变质基性火山岩 LA-ICP-MS 锆石 U-Pb 年龄及其地质意义. 地质通报, 31(1): 264 ─276

张士贞, 李奋勇, 李勇, 刘伟, 秦雅东. 2014. 雅鲁藏布江结合带中段早奥陶世强过铝质花岗岩的厘定及其地质意义. 中国科学(地球科学), 44(7): 1388 ─1402

张泽明, 王金丽, 沈昆, 石超. 2008. 环东冈瓦纳大陆周缘的古生代造山作用: 东喜马拉雅构造结南迦巴瓦岩群的岩石学和年代学证据. 岩石学报, 24(7): 1627 ─1637

张泽明, 董昕, 贺振宇, 向华. 2013. 喜马拉雅造山带的高压超高压变质作用与印度-亚洲大陆碰撞. 岩石学报, 29(5): 1713 ─1726